# A Satellite-Based Climatic Description of Jet Aircraft Contrails and Associations with Atmospheric Conditions, 1977–79

JAMES Q. DEGRAND

*Department of Geography, The Ohio State University, Columbus, Ohio*

ANDREW M. CARLETON

*Department of Geography and Earth System Science Center, The Pennsylvania State University, University Park, Pennsylvania*

DAVID J. TRAVIS

*Department of Geography, University of Wisconsin—Whitewater, Whitewater, Wisconsin*

PETER J. LAMB

*Cooperative Institute for Mesoscale Meteorological Studies, and School of Meteorology, University of Oklahoma, Norman, Oklahoma*

(Manuscript received 24 May 1999, in final form 23 September 1999)

ABSTRACT

The possible contribution of jet aircraft condensation trails (contrails) to recent observed increases in high cloudiness constitutes a potentially important human effect on climate that has received relatively little attention. Very high resolution (0.6 km) thermal-infrared imagery from the Defense Meteorological Satellite Program polar orbiters, concentrated in the nighttime and morning hours, is interpreted to derive a climatic description of contrails over the United States and adjacent areas for the midseason months (April, July, October, and January) of 1977–79. A manual technique of identifying contrails on the imagery is validated by comparison with more recent ground-based observations. Contrail spatial distributions are mapped at a 1° lat × 1° long resolution for monthly and multimonth time periods.

Contrail incidence is widespread over the United States and adjacent areas, with highest frequencies occurring over the following regions: the extreme Southwest (particularly southern California), the Southeast (especially southeast Georgia and northeast Florida), the west coast of British Columbia and Vancouver Island, and the eastern Midwest centered on southeast Indiana and western Kentucky. Contrails are most frequent during the transition-season months (April and October), and are least frequent in July. Latitudinally, contrail incidence peaks over the northern (southern) regions in July (January), suggesting a first-order association with the seasonal variation of upper-tropospheric westerly winds. Analysis of synoptic-scale midtropospheric circulation patterns confirms that the highest contrail frequencies occur in association with baroclinic phenomena, particularly cyclone waves and jet streams. Moreover, contrails tend frequently to occur in conjunction with other clouds, including the cirrus associated with jet-stream and frontal systems.

Analyses of rawinsonde data for three representative contrail ''outbreak'' (multiple occurrence) events during the study months confirm some earlier studies that suggest contrails form below a cold, elevated tropopause (i.e., around ridgelines in the geopotential height field), in contrast with noncontrail days. Accordingly, the temperature advection in the troposphere accompanying the contrail outbreaks is positive, or warm, and relatively weak. This contrail climatic description provides a context within which recent surface climate changes at regional and subregional scales may be cast.

## 1. Introduction

The possibility that human activities are affecting regional and global climate continues to be debated vigorously (e.g., Karl et al. 1996). This debate has focused largely on changes in the composition of the atmosphere, especially the effects of increasing concentrations of ''greenhouse'' gases, the depletion of stratospheric ozone, and emissions of sulfate aerosols (e.g., Plantico et al. 1990; NASA/NOAA/UKDOE/UNEP/WMO 1991; Hunter et al. 1993; Parungo et al. 1994). Human activities also may be changing other features of the atmosphere, however, most notably its cloudiness

*Corresponding author address:* Dr. Andrew M. Carleton, Dept. of Geography, The Pennsylvania State University, 302 Walker Bldg., University Park, PA 16802.
E-mail: carleton@essc.psu.edu

(Karl and Steurer 1990; Henderson-Sellers 1992). Because clouds are the most important factor determining the amount and variability of radiant energy received by the earth–atmosphere system and reradiated to space (Arking 1991; Wielicki et al. 1995), any widespread change in the quantity or nature of clouds (e.g., their mean amount, optical thickness, cloud-top temperature) could affect climate by modifying the radiation budget and global atmospheric circulation (Sohn and Smith 1992a,b; Tselioudis and Rossow 1994; Twohy et al. 1995). Moreover, the question of greenhouse gas–induced global warming is likely to be linked to, and could even be opposed by, large-scale changes in cloud properties (e.g., Lawrence 1993; Molnar 1993; Tselioudis et al. 1993; Platnick and Twomey 1994).

Atmospheric pollution by human activities may affect cloud feedbacks either by modifying existing clouds, as in the case of ''ship trails'' observed within marine stratus (Coakley et al. 1987; Radke et al. 1989; Ackerman et al. 1995), or by generating new clouds. The upper-level (about 10–12-km altitude) ice crystal clouds produced by jet aircraft and known as contrails (condensation trails), or ''false cirrus,'' exemplify this latter effect (Appleman 1953; Hall 1970; Scorer 1978, chapter 11.3; Boin and Levkov 1994; Hanson and Hanson 1995). They also may help to extend the ''natural'' cirrus cover in adjacent areas where relative humidities may be too low for spontaneous nucleation of ice crystals (Heymsfield et al. 1998). Contrails may affect the atmospheric moisture budget by ''scavenging'' large cloud particles from the upper troposphere (Hudson and Xie 1998) and by ''seeding'' clouds at lower altitudes (Harami 1968). Because contrails are less restricted spatially than ship trails (e.g., Travis et al. 1997; Minnis et al. 1997), they have the potential to influence the climate where humans live (Changnon 1981; Grassl 1990; Strauss et al. 1997; Sassen 1997).

Continental-scale increases in cloud amount have occurred during this century (e.g., Henderson-Sellers and McGuffie 1989; Henderson-Sellers 1992; Kaiser and Razuvaev 1995). Between 1950 and 1988, a widespread significant increase (+3.7%) in total cloudiness for the United States was not matched by a significant decrease (−0.9%) in possible sunshine (Angell et al. 1984; Angell 1990), suggesting thin cirrus to be the main contributor, possibly from contrails (e.g., Machta and Carpenter 1971; Changnon 1981; Lee and Johnson 1985; Seaver and Lee 1987; Liou et al. 1990). Although some of these cloud-cover increases and sunshine decreases predate the widespread increase in jet air traffic that occurred during the 1960s (Karl and Steurer 1990; Henderson-Sellers 1992), changes in instrumentation (sunshine) and observing practices (cloud) may be important in those pre-1960s cases (Cerveny and Balling 1990; Plantico et al. 1990). Increased cirrus-level cloudiness has been detected in climate data for stations in the midwestern and northeastern United States that are located beneath the major upper-tropospheric flight paths but not for stations on either side (Changnon 1981; Allard 1997).

The difficulty in ascribing some recent cloud-cover increases to contrails results from both the large natural variability of climate and clouds (Cairns 1993; Croke et al. 1999) and the lack of spatially reliable documentation of contrail frequencies, at least until very recently (cf. Minnis et al. 1997). Bryson and Wendland (1975) estimated that contrails may have increased the cirrus cloud cover over North America by 5%–10% since the early 1960s; their calculations assumed that 50% of all flights produce contrails that persist for at least 2 h, however. Although this percent is likely an overestimate, the ability to observe contrails from the surface (e.g., Wendland and Semonin 1982) is influenced heavily by the presence of lower clouds and is limited to the region around the observing site. These limitations are similar to those attending the derivation of cirrus-cloud climate descriptions using surface observations (e.g., Mazin et al. 1993). Even so, surface-based observations of sky cover for U.S. locations characterized by a high frequency of jet traffic, for days on which the upper cloud fraction can be viewed, repeatedly give ''contrail-day'' frequencies of about 30% per month (Knollenberg 1972; Wendland and Semonin 1982; Detwiler and Pratt 1984; Minnis et al. 1997). Furthermore, aircraft-level observations (e.g., Changnon et al. 1980; Detwiler and Pratt 1984) as well as those observations made using satellites (Engelstad et al. 1992; Travis 1996a), show that contrails are considerably more common and may be more persistent when other (natural) clouds occur rather than when the sky is otherwise clear (see also DeGrand 1991; Minnis et al. 1997; Mannstein et al. 1999). This finding implies that the incidence of contrails suggested by surface-level observations has been underestimated, along with their likely climatic impacts.

A climatic role for contrails, like those of natural cirrus clouds, derives from their high altitude, composition, and wide range of thicknesses. These variables affect the contrail solar reflectivity and absorption characteristics along with the IR emissivity (e.g., Liou 1986; Platt 1989; Dowling and Radke 1990; Liou et al. 1990), and also make contrails detectable in satellite observations with these wavelengths. Differences occur in the microphysics of contrails versus those of natural cirrus, especially the ice crystal size and concentration (Kuo et al. 1988; Sassen 1991; Gothe and Grassl 1993; Brogniez et al. 1995; Gayet et al. 1996; Hudson and Xie 1998; Poellot et al. 1999). The exact effect of these differences is uncertain, although an improved understanding has resulted from the Subsonic Aircraft: Contrail and Cloud Effects Special Study program conducted over the central and western United States during April–May 1996 (e.g., Jensen et al. 1998; Liou et al. 1998; Schulz 1998). Contrails occurring in the daytime may reduce the surface receipt of solar radiation more than they enhance the IR back radiation, especially when the contrails are relatively new and thick (Reinking

1968; Nicodemus and McQuigg 1969; Kuhn 1970; Jacobs 1971; Schumann and Wendling 1990; Mims and Travis 1997; Sassen 1997; Khvorostyanov and Sassen 1998), because they contain a greater density of small ($<10$ $\mu$m radius) particles at this time (Duda et al. 1998; Liou et al. 1998). Contrails that attain greater horizontal extent over multihour timescales (Minnis et al. 1998), however, tend to become thinner and behave more like natural cirrus as their cloud particle sizes increase (Duda et al. 1998). Thus, persistent contrails may exert a positive ''cloud-radiative forcing'' (Manabe 1975; Freeman and Liou 1979; Detwiler 1983; Grassl 1990; Parol et al. 1991; Poetzsch-Heffter et al. 1995; Mannstein et al. 1999). This forcing would result in either a mean surface temperature increase or a reduced diurnal temperature range because of elevated overnight minimum temperatures (Liou et al. 1990; Travis 1996a), possibly differentiated according to season (Fortuin et al. 1995; Ponater et al. 1996).

Persisting contrails represent the visible condensate of water vapor injected into the upper troposphere by jet aircraft and also sublimated from the environment (Schumann 1996; Chlond 1998). Thus, contrails represent a subset of the total effect of subsonic aircraft on the tropospheric moisture budget: that from visible cloud formation. This effect is separate from the contribution of emitted water vapor (Rind et al. 1996) or of contrails that are subvisual and optically thin (Sassen et al. 1989; Hutchison et al. 1995; Wang et al. 1996). GCM experiments investigating the relative contributions globally of contrails and aircraft water vapor emissions (Ponater et al. 1996) suggest that the contrail cloud radiative forcing far exceeds that from the additional water vapor for current air traffic patterns and also those predicted to occur in the near future (see also Rind et al. 1996). Accordingly, modeling and observational studies of the likely climatic effects of jet aircraft activity in the troposphere emphasize the role of contrails (Liou et al. 1990; Fortuin et al. 1995; Strauss et al. 1997; Poellot et al. 1999). As a prerequisite for determining more precisely the effects of jet contrail cirrus on the radiative and thermal climate of the lower troposphere and the earth's surface, reliable information on the frequencies of occurrence of contrails and their spatial and temporal variability is clearly required.

Satellite data are largely free from the biases inherent in observing contrails from the ground or from aircraft. The linear appearance of contrails soon after formation and their occurrence as ''outbreaks'' in fields with length scales of 1000 km or longer (Bakan et al. 1994; Travis et al. 1997) makes them readily identifiable in higher-resolution satellite imagery (e.g., Joseph et al. 1975; Detwiler and Pratt 1984; Carleton and Lamb 1986; Lee 1989; Schumann and Wendling 1990; Mannstein et al. 1999). In particular, Bakan et al. (1994) used the 1.1-km-resolution National Oceanic and Atmospheric Administration (NOAA) Advanced Very High Resolution Radiometer (AVHRR) IR images to derive a 2-yr climate description of jet contrails over Europe and the eastern trans-Atlantic air corridor (30°W–30°E, 35°–75°N). These authors give a value for the yearly average contribution by contrail cloudiness of almost 2% regionally. This contribution is the same as that suggested by Grassl (1990) to be as important to the radiation budget as a 10% increase of the present anthropogenic $CO_2$ forcing. The European regional-scale contrail study by Mannstein et al. (1999), however, covering a different period and using an automated detection method for contrails, gives an annual mean contrail coverage of only 0.5% $\pm$ 0.25%. It would be highly useful to compare the results of these authors with the other continental region characterized by high frequencies of jet air traffic, namely, the United States and surrounding regions (e.g., Ponater et al. 1996, their Fig. 1; Rind et al. 1996, their Fig. 2; Minnis et al. 1999, their Fig. 1).

The contrail climatic description presented for the conterminous United States and adjacent ocean areas is developed using very high resolution ''direct-readout'' (DR) images from the Defense Meteorological Satellite Program (DMSP) satellites. The climate description is for the midseason months (January, April, July, October) of the years 1977–79, and is mapped at spatial resolutions of 1° lat $\times$ 1° long. This mapped resolution of contrail frequency is much finer than that used by Bakan et al. (1994), which was 10° long $\times$ 5° lat. The contrail dataset enables addressing of the following aspects of contrails: 1) their dominant spatial and seasonal patterns of occurrence, 2) their associations with mid- to upper-tropospheric meteorological conditions and with the patterns of synoptic-scale atmospheric circulation, and 3) their associations with naturally occurring clouds.

Information on the above characteristics of contrails provides the necessary context for investigations that seek to evaluate better the presence of a contrail signal in U.S. climate station data and its role vis-à-vis other sources of recent climate change.

## 2. Data and analysis

### *a. DMSP imagery*

Upwelling radiation in the thermal-IR window and solar wavelengths is recorded by the DMSP polar orbiters and transmitted continuously to U.S. military installations worldwide in DR form. In the continental United States, the data are acquired by two reception installations at Patrick Air Force Base (PAFB), Florida, and San Diego Naval Base (SDNB), California, and archived at the National Snow and Ice Data Center in Boulder, Colorado. Although there is no DMSP digital archive available before the early 1990s, the hard-copy images used here have a nominal resolution of 0.6 km (e.g., Fig. 1), which is slightly better than the 1.1-km resolution of AVHRR (cf. Bakan et al. 1994). Contrail studies that used Landsat multispectral scanner system

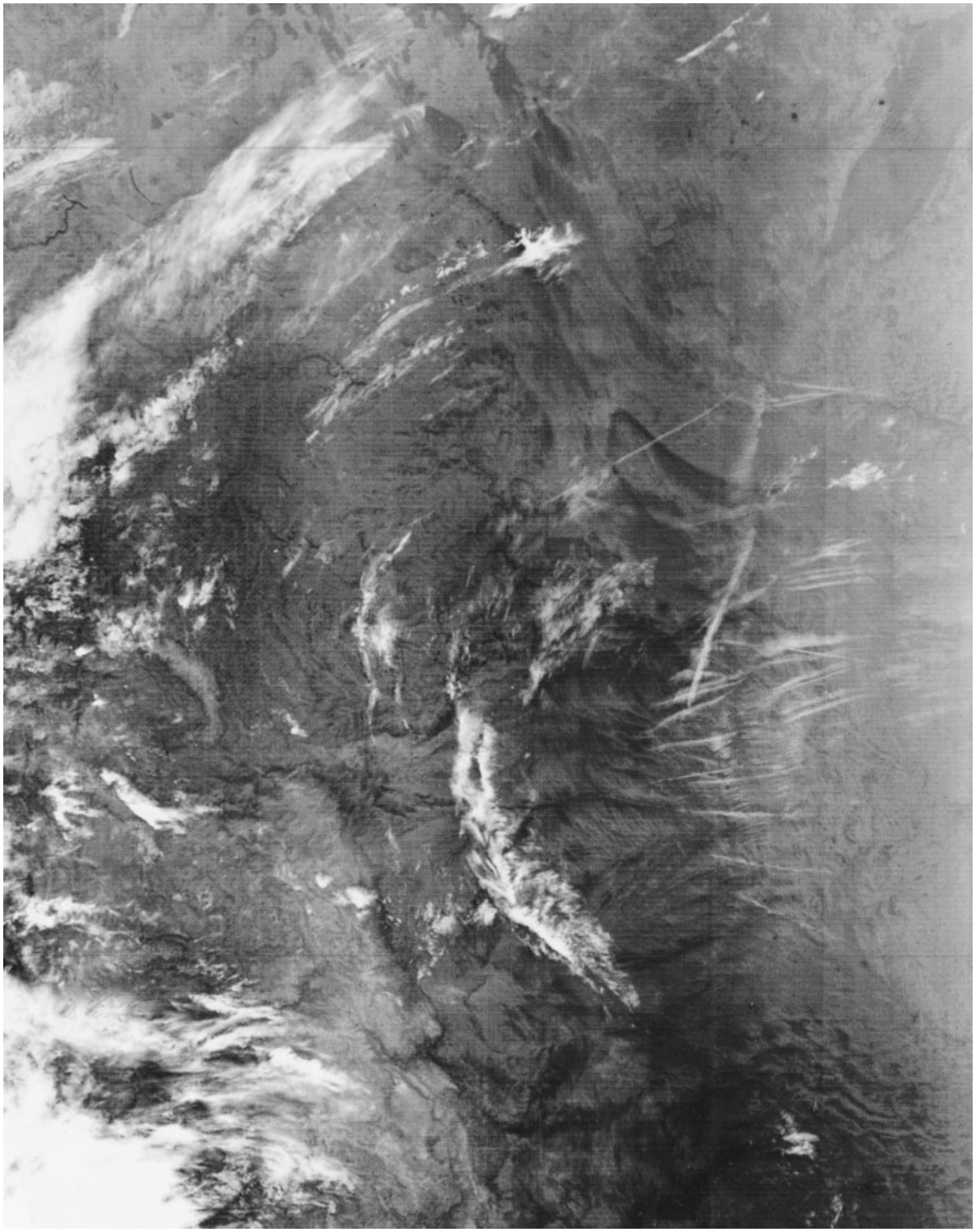

FIG. 1. DMSP DR thermal-IR image acquired by SDNB at 0310 UTC 20 Oct 1977. The imaged area is the western Great Plains of the United States, with Lake Superior and Lake Winnipeg evident in the upper-right and upper-center portions of the image. Twenty-four west–east-oriented contrails associated with patchy cirrus and with clear air were identified over eastern portions of South Dakota and Nebraska and western portions of Minnesota and Iowa (right-hand side of center part of image). The long contrail oriented south-southwest to north-northeast and bisecting the other shorter contrails shows evidence of spreading, diffusion, and thinning.

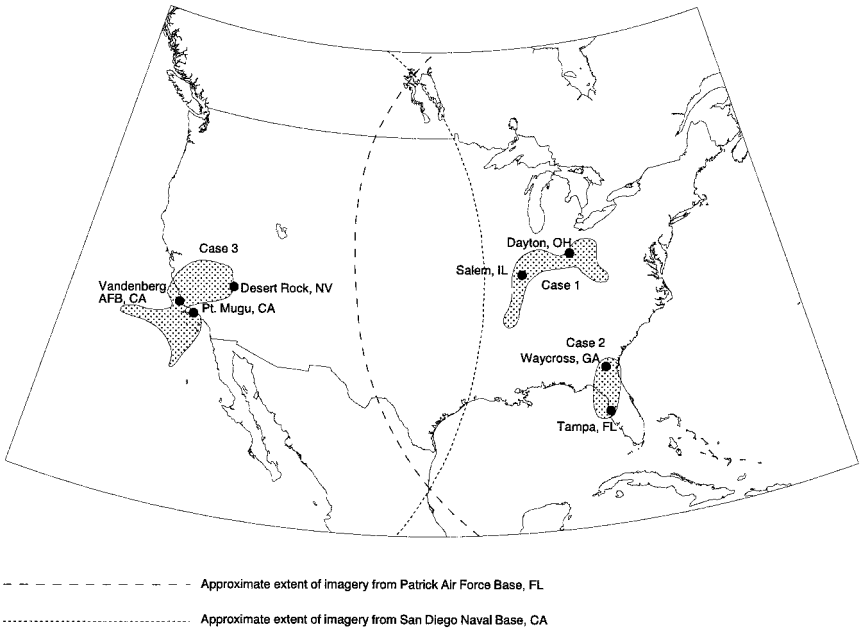


FIG. 2. Map showing approximate coverages of the DMSP DR data for PAFB (area eastward of dashed line) and SDNB (area westward of dotted line) in relation to the study area (apron-shaped area extending from southern Canada to central Mexico and including parts of the eastern Pacific and western Atlantic Oceans). Also included are the locations of three contrail outbreak cases (shaded) and rawinsonde stations used to provide thermodynamic information on the contrails involved (see section 4). Case numbers pertain to Table 3.

data at 80 m × 80 m resolution report typical contrail widths of 1–2 km (Joseph et al. 1975; Detwiler and Pratt 1984). Accordingly, the 0.6-km resolution of the DMSP DR imagery is capable of resolving contrail-scale cloud features about 90% of the time (Detwiler and Pratt 1984), provided that these clouds are sufficiently thick (i.e., are not subvisual). Thus, the satellite data are detecting primarily ''persistent linear contrails'' (Minnis et al. 1998) rather than contrails that may be short-lived or narrow or may have become too diffuse through lateral spreading to be detected. The ungridded and unrectified Mylar image transparencies are at a nominal scale of 1:15 000 000. The DR images are highly appropriate for developing a contrail dataset because of their extensive spatial coverage of the United States and inclusion of large areas of southern Canada, northern Mexico, and the eastern Pacific and western Atlantic Oceans (the outlined areas shown on Fig. 2).

TABLE 1. Numbers of images available for analysis and numbers of days represented in the DMSP DR archive for PAFB and SDNB for the 11-month study period.

| | PAFB | | SDNB | |
|---|---|---|---|---|
| Month/year | Images | Days | Images | Days |
| 4/77 | 20 | 15 | 28 | 16 |
| 7/77 | 35 | 18 | 41 | 28 |
| 10/77 | 46 | 20 | 54 | 31 |
| 1/78 | 43 | 20 | 49 | 29 |
| 4/78 | 33 | 18 | 56 | 30 |
| 7/78 | 56 | 22 | 44 | 26 |
| 10/78 | 52 | 22 | 51 | 26 |
| 1/79 | 55 | 19 | 44 | 28 |
| 4/79 | 44 | 19 | 53 | 30 |
| 7/79 | 15 | 9 | 72 | 31 |
| 10/79 | 63 | 22 | 59 | 30 |
| Total | 462 | 204 | 551 | 305 |

The period 1977–79 had the maximum availability of DMSP DR data from both U.S. Air Force sites prior to initiation of this study in 1990. The time-intensive nature of identifying contrails on the hard-copy images necessitated that the contrail climatic description be developed for midseason months only (January, April, July, October), but this resolution adequately captures the annual variations of contrail occurrence in relation to the dominant annual cycle of the larger-scale atmospheric circulation over middle latitudes. Thus, the 11 midseason months from April 1977 through October 1979 (the ''study period'') provide the only such months that are ''sequential'' and for which extensive amounts of data are available (Table 1). The months and years selected are generally representative of the longer-term mean monthly atmospheric circulation patterns, although the two Januaries analyzed here (1978 and 1979) may be somewhat less representative because of their unusually large negative 700-hPa height anomalies and low temperatures over the central and eastern United States (Wagner 1978, 1979).

Persistent linear contrails were detected using the thermal-IR (8–13 $\mu$m through June 1979, 10.4–12.5 $\mu$m

thereafter) images, rather than the simultaneous solar (0.5–0.9 $\mu$m)–band (visible, or VIS) imagery, because the approximate altitude of cloud features can be ascertained from their equivalent blackbody temperature (Carleton and Lamb 1986). This approach avoids confusing contrails with other features such as ship tracks and boundary outflows (Fett and Mitchell 1977) that might occur when using the VIS data. Although the blackbody assumption for clouds in the IR window region is problematic for cirrus and contrails (e.g., Brogniez et al. 1995), this effect is unlikely to be a major source of error in the current manually derived climatic description. The linear nature and extremely low cloud-top temperatures (typically $<-40$°C) characteristic of contrails that have not spread or become diffuse contrast strongly with the underlying surface or lower and warmer clouds upon which they may be superimposed.

The minor disadvantages of the DMSP DR images for developing a contrail climatic dataset are outweighed by the above-mentioned advantages of spatial coverage, resolution, and period of record. The minor drawbacks include a reduction in the number of images (to two or three per DR site per day) from the maximum possible (four) on about 75% of days. This reduction is due to the primary DMSP objective being weather forecasting rather than climate monitoring. There is also a bias toward imagery for the nighttime and morning hours. Ninety-eight percent of all images were recorded between 0000 and 1800 UTC (i.e., 1900–1300 EST; 1600–1000 PST), and only 2% were recorded between 1800 and 0000 UTC (i.e., 1300–1900 EST; 1000–1600 PST). Thus, most of the data are for times when commercial air traffic over the United States is at a minimum (Federal Aviation Administration 1979; Minnis et al. 1997), and the contrail frequencies obtained in this climatic dataset therefore are likely to be lower than for the diurnal period as a whole (see also Bakan et al. 1994; Mannstein et al. 1999). These limitations of the DMSP DR imagery also meant that it was not possible to evaluate the persistence and spreading characteristics of jet contrails that some studies consider also to be climatically important (Kuhn 1970; Joseph et al. 1975; Wendland and Semonin 1982; Mannstein et al. 1999). Such an undertaking requires data at much higher temporal resolutions than those available here.

### *b. Contrail identification and comparisons with other contrail observations*

Contrails were identified on the imagery as linear, bright (i.e., cold in IR) clouds with lengths typically ranging from 10 to 100 km and orientations that often were different from those of neighboring natural cirrus (e.g., see the contrails present in Fig. 1; Carleton and Lamb 1986; Bakan et al. 1994). This definition sought to prevent the misclassification of natural cirrus streamers as contrails and was assisted by the tendency for contrails to occur as outbreaks in areas of heavy jet traffic (Wendland and Semonin 1982; Detwiler and Pratt 1984; Carleton and Lamb 1986; Liou et al. 1990; Bakan et al. 1994). Because the difference in appearance between a contrail and natural cirrus is greatest when the contrail initially forms or in the absence of appreciable wind shear (Lee 1989; Engelstad et al. 1992; center-right of current Fig. 1), it is likely that application of the criteria used to identify contrails was successful in excluding natural cirrus from the database for especially the early stages of contrail development. Some older contrails likely were not included because of their greater resemblance to natural cirrus as spreading occurs, which is a problem shared by many automated contrail detection methods applied to digital satellite data (Engelstad et al. 1992; Mannstein et al. 1999).

The absence of a routine surface-based observing network for contrails and the frequent obscuration of the high-cloud fraction by intervening cloud layers make it difficult to obtain independent verification of this subjective method of identifying contrails on the satellite imagery. We attempted such a check by comparing surface-based observations of contrails taken at Bloomington, Indiana, with those identified using *NOAA-12* AVHRR 1.1-km-resolution satellite images of southern Indiana, for a more recent time period (Travis 1994). Surface observations of contrails and natural cloud cover were recorded each day at approximately 0800 local time by D. Travis for the months of September, October, and November 1993. The sky condition, percentage of sky coverage by contrails (if any), and their dominant sky quadrant, as well as any apparent tendency for contrails to be spreading, were recorded. Both single contrails and outbreaks were noted, the latter defined as contrails covering at least 10% of the sky. All available hard-copy AVHRR IR image swaths were inspected for contrails over south-central Indiana using the same criteria as are used in the current larger study of the DMSP DR data. Of the 91 days, there were only 22 for which no satellite images were available.

Figure 3 confirms the ability of the subjective technique to identify contrails on higher-resolution imagery. There is good agreement between the number of contrail outbreaks recognized from the surface and on the simultaneous satellite image (Table 2). Moreover, the satellite technique is superior to surface observations as cloud cover increases. Contrail outbreaks were evident on the AVHRR images but not from the corresponding surface observations for six times, all of which occurred with completely overcast conditions at Bloomington. Contrails were evident from the surface but not from satellite on only 2 days in the 3-month period. The field notes for these 2 days indicate that, although contrails were observed, they appeared not to be spreading, which may explain the inability to detect them on the 1.1-km-resolution satellite images.

A second check of the analysis method used to develop the current contrail climatic description involved J. DeGrand (1991) independently reanalyzing the DR

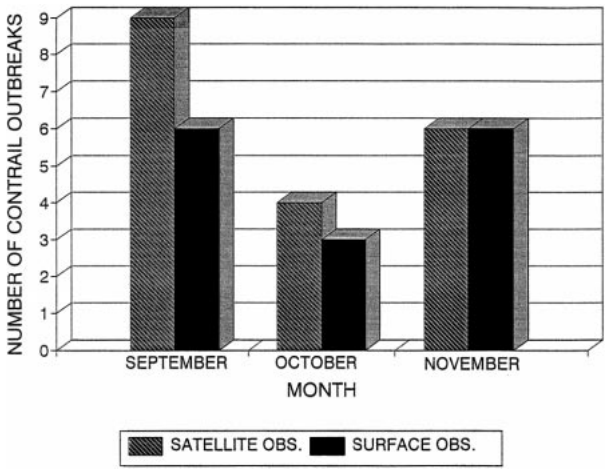


FIG. 3. Contrail outbreak frequencies by month (Sep, Oct, and Nov of 1993) for Bloomington, south-central Indiana, as observed from the surface and on *NOAA-12* images.

data for the same month (October 1978) studied by Carleton and Lamb (1986, their Table 2), and comparing the results. Contrails identified on the images by Carleton and Lamb also were identified by DeGrand in 75% of cases. For those images on which both researchers identified contrails, the *locations* of those contrails agreed in 89% of cases, which supports the more conservative approach to contrail identification adopted by DeGrand in the current larger study.

## 3. Contrail climatic description

### *a. Mean patterns and annual variations of contrails*

In mapping the mean calendar monthly and composite (11-month) distributions of persistent linear contrails for the conterminous United States and adjacent ocean regions, it was necessary to correct for spatial and temporal variations in the DMSP DR image frequency and coverage. This correction was done by expressing the number of contrails identified for each $1° \times 1°$ grid cell as a percentage of the number of available images. Although satellite-based contrail studies for Europe (Bakan et al. 1994; Mannstein et al. 1999) present maps of the additional cirrus coverage from contrails, essentially by spatially smoothing the frequencies of linear contrails, our preference in this study is to retain the high spatial resolution afforded by the DMSP DR imagery. The question of the propensity for individual contrails to transform into cirrostratus (cf. Sassen and Hsueh 1998) is left to subsequent studies, because such an undertaking requires data at higher temporal resolution than those available here (e.g., Minnis et al. 1998).

Figure 4 shows the spatial distribution (plotted on an equal-area projection) of contrails for all 11 study months, normalized to image frequency. Contrails are a widespread phenomenon over the United States and adjacent waters and were observed in 1039 of the 2376

TABLE 2. Comparison of surface and satellite observations of contrail outbreaks over Bloomington, south-central Indiana, Sep–Nov 1993. The chi-square value of 33.9 (significant at $p < 0.01$) indicates that the agreement between the satellite and surface observations (both ''yes'' or both ''no'') is statistically significant.

| Satellite identification of contrails | Surface identification of contrails | |
|---|---|---|
| | Yes | No |
| Yes = 19 | 13 | 6 |
| No = 50 | 2 | 48 |

grid cells in the study area (44%) at some time during the 11 study months. Of the 1039 grid cells in which contrails were observed, 805 (78%) were located in the latitude band between 28.5° and 46.5°N. There is a strong regional dependence to contrail occurrence (Fig. 4), with highest frequencies occurring in the following regions: 1) the southwestern United States, especially southern California; 2) the southeastern United States (specifically southeastern Georgia and north-central Florida); 3) the coast of British Columbia, including Vancouver Island; and 4) the midwestern United States centered over southeastern Indiana and western Kentucky. In general, contrails were observed infrequently over the northern and southern extremes of the study area and the intermountain areas of the western United States. For the study region as a whole, contrail incidence peaks during the transition months (April and October) at values that are 109% and 111%, respectively, of the mean value of contrail incidence for all midseason months (Fig. 5). In April and October, also, the latitude band of maximum frequency comes from the middle of the 29°–46°N zone and not further north or south. The maximum in October results largely from the high frequencies for October 1979 (Fig. 6). Contrail incidence over the United States is at a minimum during July (Figs. 5 and 6), when it is 80% of the mean value.

The number of contrails observed for any one grid cell in Fig. 4 appears to be low considering the large volume of air traffic over much of the study area (Changnon 1981) and when compared with the Europe/eastern North Atlantic contrail study by Bakan et al. (1994). This difference likely results from combinations of factors, particularly the preponderance of nighttime and morning images in the DMSP DR archive. Bakan et al. (1994) found that contrail cloudiness over Europe and the eastern North Atlantic is about twice as high during the day as compared with the nighttime hours. The day–night difference is virtually threefold in the European regional study by Mannstein et al. (1999). Minnis et al. (1997) report a midmorning maximum of contrails observed from the ground at military stations in the United States. In addition, the current contrail dataset is representative of the period just preceding major deregulation of the U.S. airline industry. Air traffic subsequently increased by about 5%–6% per year, with jet fuel consumption increasing by only about 3% per year (Schumann 1994), the latter reflecting the im-

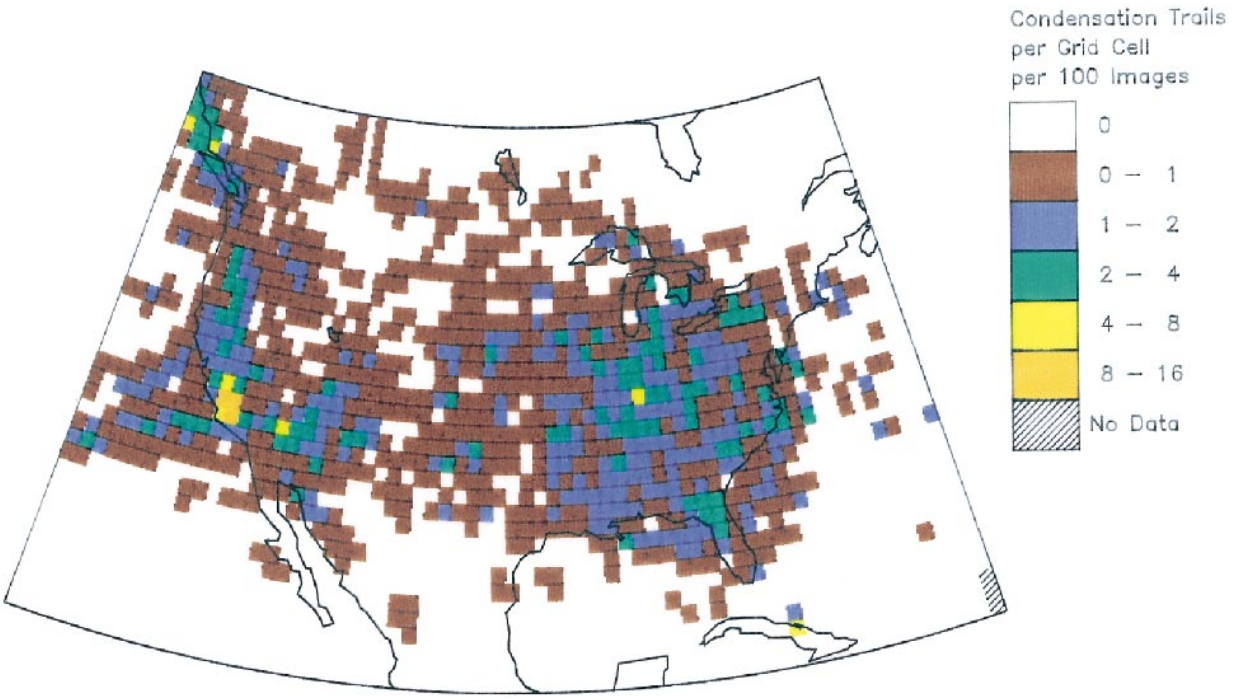


FIG. 4. Summary map for all 11 months of the study period, showing normalized frequencies of contrails per grid cell per 100 images.

proved efficiency of jet engines. Supporting evidence for a reduced number of contrails in the current study period relative to the 1980s and 1990s comes from Minnis (1998, personal communication). He has compared statistically our satellite-derived frequencies of contrails for 1977–79 with those observed from the ground for the period April 1993 through April 1994 and infers that the frequency of ''persistent'' contrails has increased by about 60% during the intervening period.

A latitudinal migration of contrail incidence between seasons (Fig. 5) is implied by the out-of-phase patterns between the more southern latitude bands (20°–29°N,

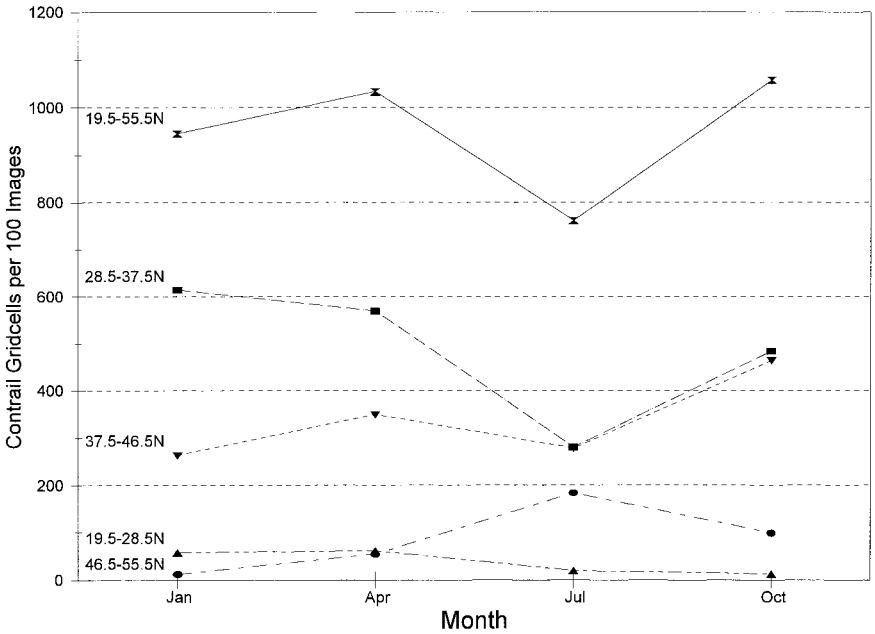


FIG. 5. Area-adjusted values of the normalized number of 1° × 1° gridcell contrail occurrences for composite midseason months by latitude zone and for the entire study area (20°–55°N).

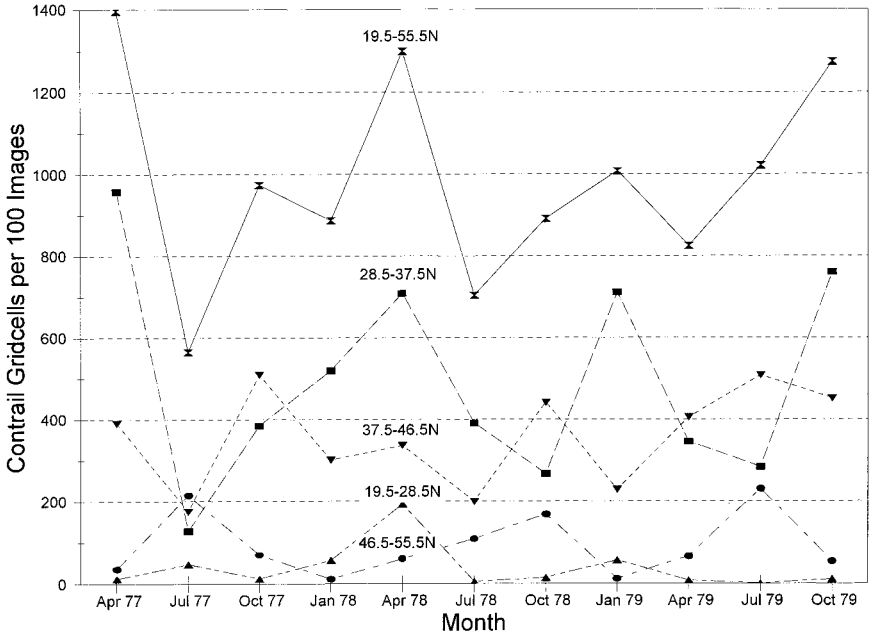


FIG. 6. Similar to Fig. 5 but for each midseason month in the study period.

29°–37°N) and the northernmost band (47°–55°N). The southern (northern) bands have peak frequencies in the midseason months representative of the colder (warmer) times of year, suggesting a dominant control by the atmospheric circulation. This control involves particularly the zonal westerlies and jet streams and their associated variations with tropopause height, temperature, and humidity (cf. Namias and Clapp 1951; Beckwith 1972; Randel et al. 1996; Peixoto and Oort 1996). A similarly strong annual variation in contrail frequencies was noted for western Europe and the eastern North Atlantic by Bakan et al. (1994).

Figure 7 complements Figs. 5 and 6 by indicating the geographical patterns of annual contrail variation. In January (Fig. 7a), the concentration of contrails over the southern half of the study area is particularly pronounced in the southeastern United States and, to a lesser extent, in the upper Midwest and far western United States. Contrails are absent over the northern and central plains, the Rocky Mountains, and southern Canada. At the other extreme, in July (Fig. 7c) contrail frequencies are decreased with respect to January over much of the southeastern United States and in the Midwest and are more concentrated along coastal British Columbia, the intermountain southwestern United States, coastal areas of southern California, and off the eastern seaboard. There also are minor increases, relative to the January pattern, scattered across the northern plains and much of southern Canada.

The transition-season months of April and October (Figs. 7b,c) show pronounced spatial differences in contrail occurrence from the seasonal extremes represented by January and July. In April (Fig. 7b), contrails are concentrated over the U.S. Southwest and eastern Midwest regions, with relatively few occurrences over the Great Plains and Rockies. In October (Fig. 7d), contrails are much more generally distributed over the United States, with slightly reduced maxima relative to July over the Southwest and eastern Midwest and an increased concentration over the south-central United States.

### *b. Interannual variations*

To examine the interannual variability of contrails and their associations with the atmospheric circulation, the following pairs of months having particularly large contrail differences in the 29°–37°N band (Fig. 6) and also spatially—October 1978 and 1979, April 1977 and 1979; and January 1978 and 1979 (Figs. 8–10a,b)—are compared. No July months are compared, because relatively few contrails occur in those months. In the absence of publicly available data on the actual flight altitudes and paths of individual commercial aircraft, the broad-scale atmospheric circulation controls on contrail development are inferred by assessing the degree to which the core areas of contrail incidence (maxima, minima) vary between the same midseason months of different years. This method is appropriate, because on these timescales little variation occurs in the broad locations of the high-altitude flight paths. The latter are depicted on published Federal Aviation Administration charts. Large variations in the mean locations and frequencies of contrails should indicate changes in the atmospheric conditions favorable for contrail development and persistence.

To evaluate the associations between the upper-tropospheric circulation and contrail frequency on a monthly basis, anomaly fields of 200-hPa geopotential height and the 250-hPa resultant vector wind (Figs. 8–10) were produced. These fields were computed from twice-daily National Meteorological Center (NMC) gridpoint analyses (NMC 1990), with reference to the mean monthly values for 1973–87. A Student's *t*-test delineated areas having differences from the 15-yr means that were statistically significant at the 95% and 99% confidence levels. This methodology is essentially the same as that undertaken by Carleton (1988). The results of this analysis are summarized in panels (c) and (d) of Figs. 8–10, which reveal large variations in the circulation between corresponding months of the years studied. From the geopotential height changes, one can infer the sign of the temperature advection (positive: warm, west of an anomalous ridge and east of an anomalous trough; negative: cold, east of an enhanced ridge and west of an enhanced trough). Spatial variations in the resultant wind speed departures also indicate anomalies in the upper tropospheric ''speed'' convergence and divergence patterns. These anomaly patterns are compared with the contrail distributions for the months in question, below.

In October 1978 (Fig. 8a), high frequencies of contrails in the interior northwestern United States and southwestern Canada contrast strongly with the absence of contrails in that region in October of the following year (1979, Fig. 8b). Conversely, in October 1979, the southwestern and south-central United States had much greater frequencies of contrails than in October 1978. A secondary continental maximum of contrails occurred in the eastern Great Lakes, and an area of higher frequencies also occurred over the eastern North Pacific Ocean off southern California in October 1978.

In April 1977 (Fig. 9a), relatively high frequencies of contrails occurred along the coastal and interior regions of California, and somewhat higher frequencies occurred in the interior southeastern United States, as compared with the corresponding regions in April 1979 (Fig. 9b). Conversely, more contrails occurred over the Great Lakes region in April 1979 as compared with April of 1977.

Although the regional changes in contrail frequencies between January 1978 and January 1979 were not as large as those for the April and October months discussed above, some differences were evident (Figs. 10a,b). In January 1978, there were fewer contrails over the northwestern United States and more contrails over the Midwest, as compared with January 1979. In January 1979, however, the contrail frequency maximum shifted to lie more strongly over the southeastern United States, as compared with January of the preceding year (also Fig. 6, 29°–37°N band).

The normalized distributions of contrails occurring on daily timescales were compared with the circulation anomaly patterns for contrasting midseason months (April 1977, 1979; October 1978, 1979; January 1978, 1979: Figs. 8–10) to determine if any general associations are evident. Regionally, higher frequencies of contrails sometimes are associated with statistically significant anomalies of upper-tropospheric wind speed (both positive and negative) and/or geopotential height. For example, the high frequencies of contrails over the northwestern United States in October 1978 and over the south-central states in October 1979 (Figs. 8a,b) occurred where the upper-tropospheric flow was anomalously weak on the cold side of upper troughs. Conversely, the large positive wind speed anomalies occurring on the warm side of an upper ridge over the U.S. Midwest and mid-Atlantic regions in April 1979 and in the California region in April 1978 were associated with higher frequencies of contrails in those months (Fig. 9b). Contrails may be less likely to occur in a region when the monthly height and/or wind anomalies are not significantly different from the climatological monthly means; for example, the south-central United States in October 1978 (Fig. 8a). This result could be from insufficient horizontal variations in either the temperature advection or wind speed convergence/divergence, both of which show some associations with contrail development on shorter (subdaily) timescales (Travis 1994, pp. 76–78; Jensen et al. 1998). The presence of significant height and wind speed anomalies in a given region is not always associated with greater frequencies of contrails on a monthly timescale, however. For example, contrails essentially are absent from the Pacific Northwest region of the United States in January 1978, yet this area had marked positive anomalies of upper-tropospheric wind speed on the warm side of an upper trough. Conversely, the same region in January 1979 had some contrails but no significant circulation anomalies. It is possible that averaging the daily contrail and circulation data on monthly scales may be at least partly responsible for the inconclusive results in these cases. To illuminate further the contrail association with atmospheric circulation, it therefore is necessary to consider each contrail observation in the context of its accompanying synoptic type (i.e., on daily timescales). This task is undertaken below and in section 4. The results of the analysis indicate a strong synoptic control on contrail occurrence.

### *c. Synoptic associations*

Contrail associations with the synoptic-scale circulation were determined using a ''subjective'' (manual) method of typing once-daily (1200 UTC; 0700 EST) midtropospheric (500 hPa) geopotential height patterns published by the U.S. National Weather Service in the Daily Weather Maps series. Although 250 hPa may have been a better atmospheric level for the synoptic typing of contrails (e.g., Beckwith 1972), it was not represented in the readily available publications used. Moreover, this use of 500 hPa should not have adversely affected the results, because, in typing the daily circulation, allow-

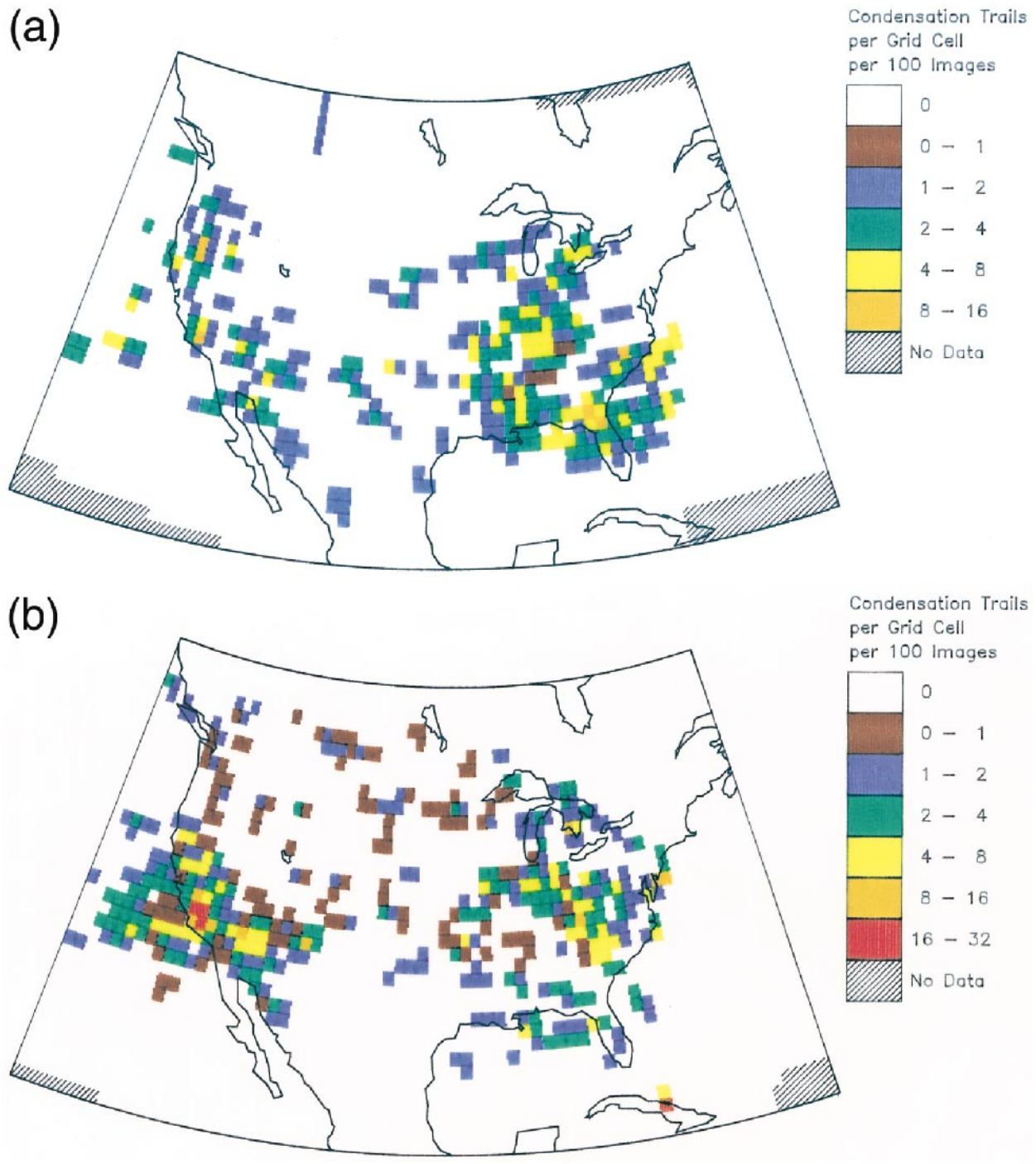


FIG. 7. Composite normalized frequencies of contrails (number per 1° × 1° grid cell per 100 images) for (a) Jan 1978, 1979; (b) Apr 1977, 1978, 1979; (c) Jul 1977, 1978, 1979; and (d) Oct 1977, 1978, 1979.

ance was made for the continuity between the mid- and upper troposphere (e.g., the slight westward slope with height of baroclinic waves, and the reduced wind speeds at 500 hPa relative to jet-stream level). The concentration of imagery in both the nighttime and morning hours (section 2a) meant that a satellite contrail observation was often for several hours earlier than its closest (in time) 500-hPa map. To accommodate this temporal offset when assigning contrails to synoptic categories, the height contours on the two consecutive 24-h maps bounding the satellite contrail observation were interpolated linearly to the time of satellite overpass.

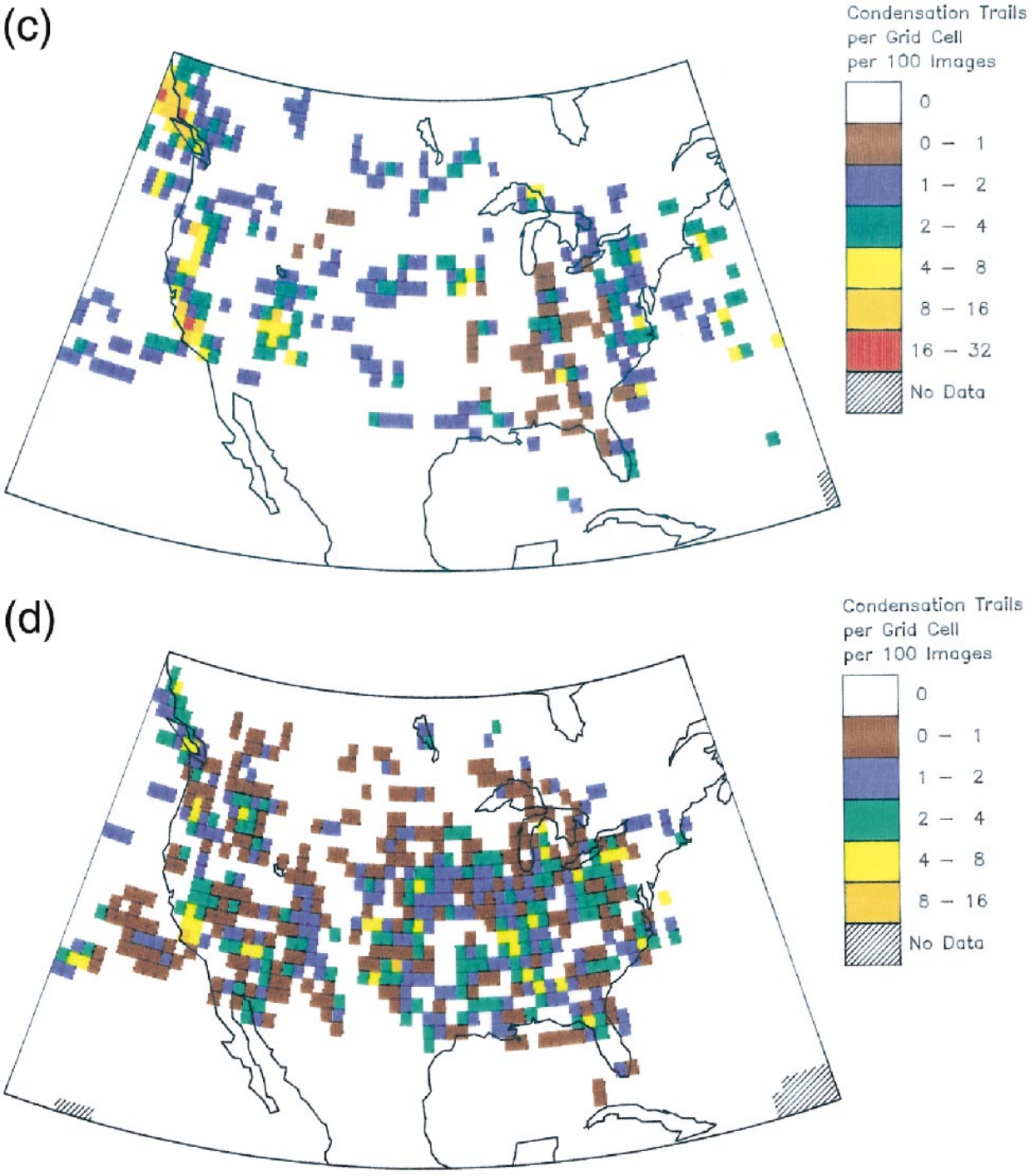


FIG. 7. (*Continued*)

The synoptic categories were developed by inspecting many daily height patterns and performing several trial classifications. The final classification scheme is very similar to that developed by Carleton and Lamb (1986) and distinguishes between circulations that are baroclinic (wave cyclone, jet stream) and those that are more barotropic (closed or zonal flow). It is as follows: 1) closed low, 2) closed high, 3) at or near a trough axis, 4) at or near a ridge axis, 5) east of a ridge/west of a trough, 6) west of a ridge/east of a trough, 7) zonal flow with a weak height gradient, 8) jet stream maximum, and 9) unclassified.

Each contrail observation on the DR imagery was assigned to the synoptic category that best reflects its

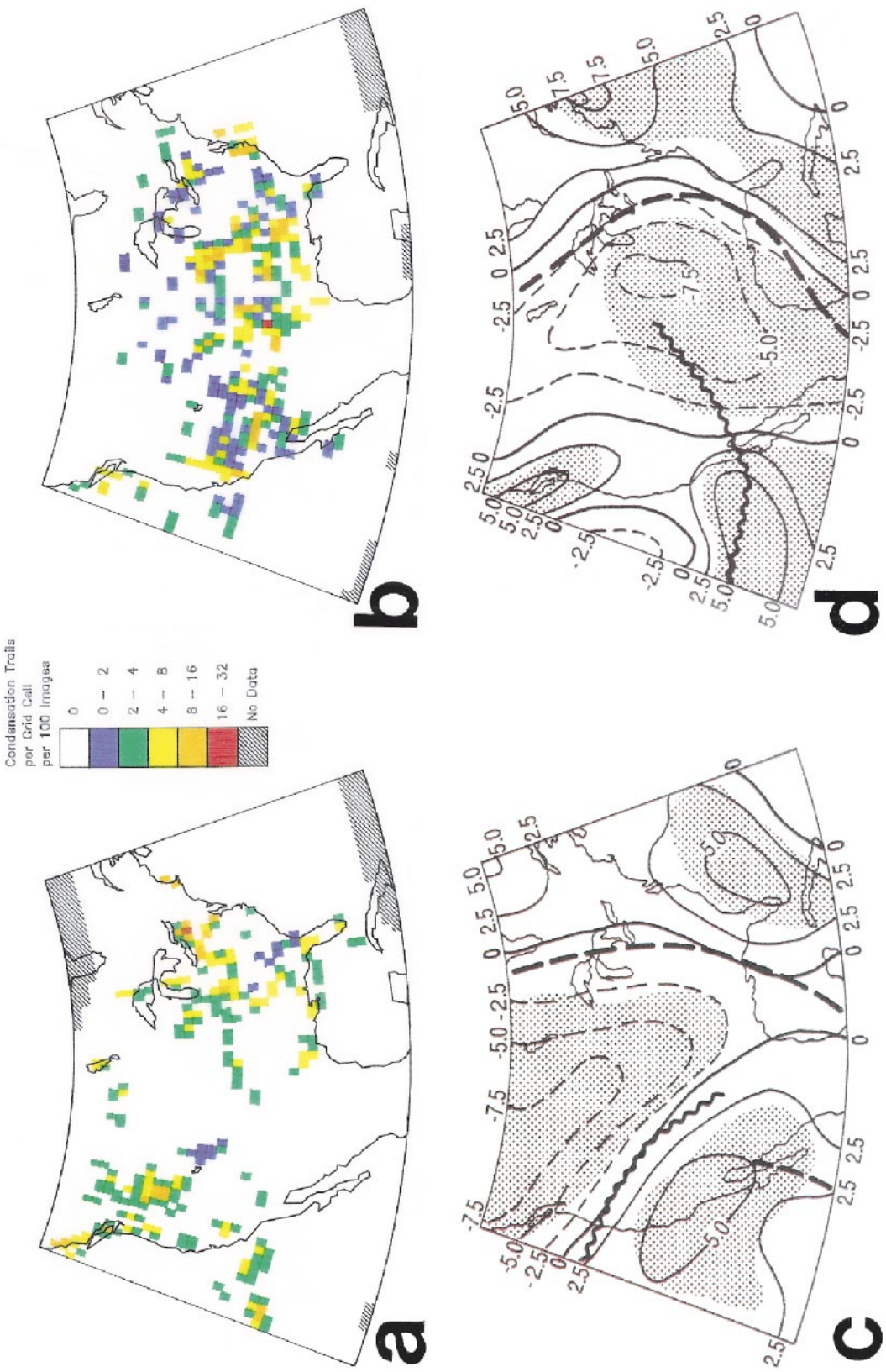


FIG. 8. Normalized frequencies of contrails (per 1° × 1° grid cell per 100 images) for the months of (a) Oct 1978 and (b) Oct 1979. Summary maps of the upper-tropospheric circulation (height and vector wind) anomalies for the same months appear in (c) and (d). The axes of statistically significant departures of monthly 200-hPa height are shown by the conventional symbols (anomalous ridge: heavy wavy line; anomalous trough: heavy dashed line). Isopleths of the monthly anomalies of 250-hPa resultant vector wind speeds at 2.5 m $s^{-1}$ intervals are shown as solid for positive (enhanced westerly) and dashed for negative (reduced westerly) departures. Shaded areas denote where the monthly departures are significantly different (at the 99% confidence level) from the 15-yr (1973–88) means for Oct.

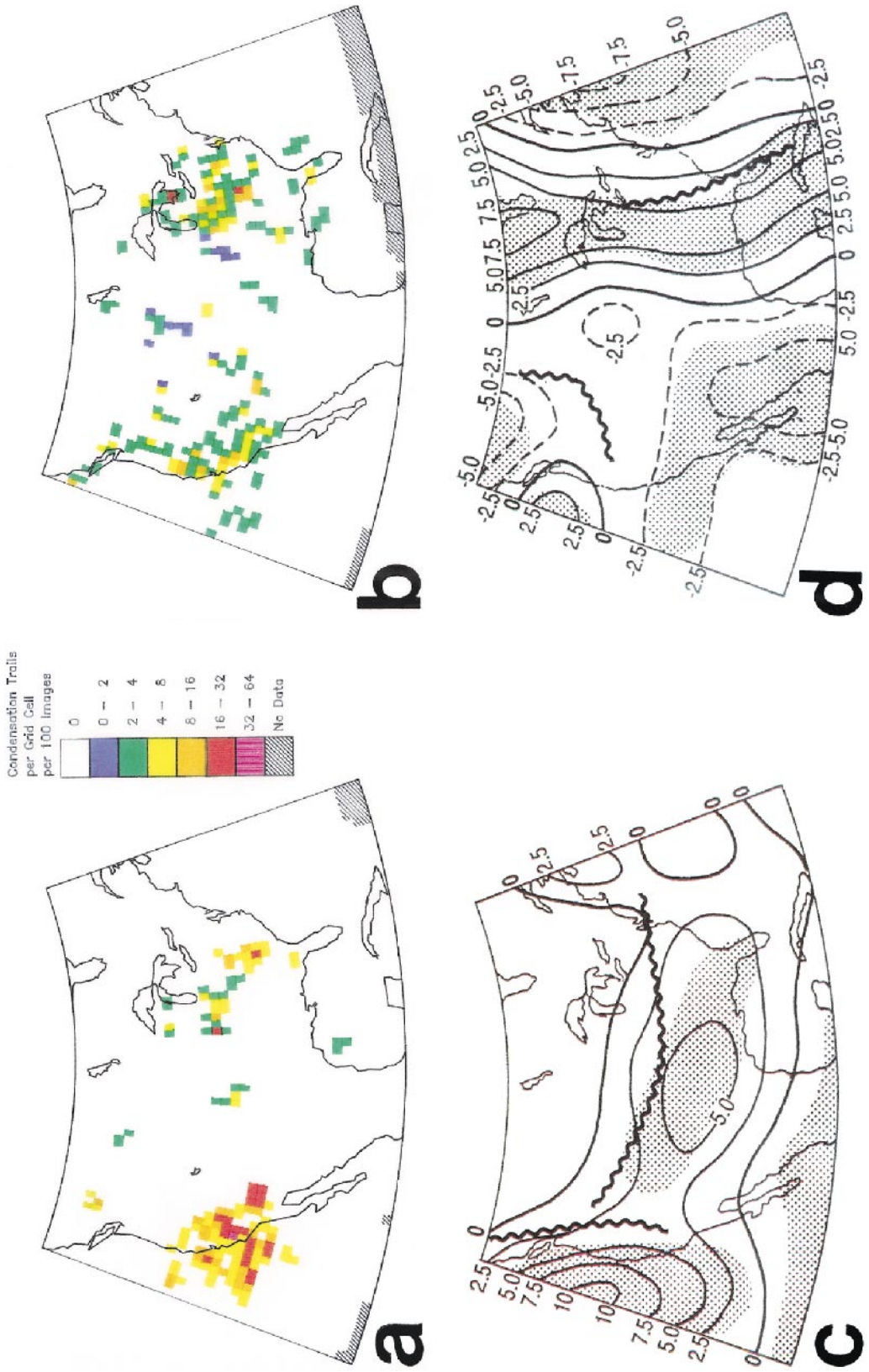


FIG. 9. Same as Fig. 8 but for (a) and (c) Apr 1977 and (b) and (d) Apr 1979.

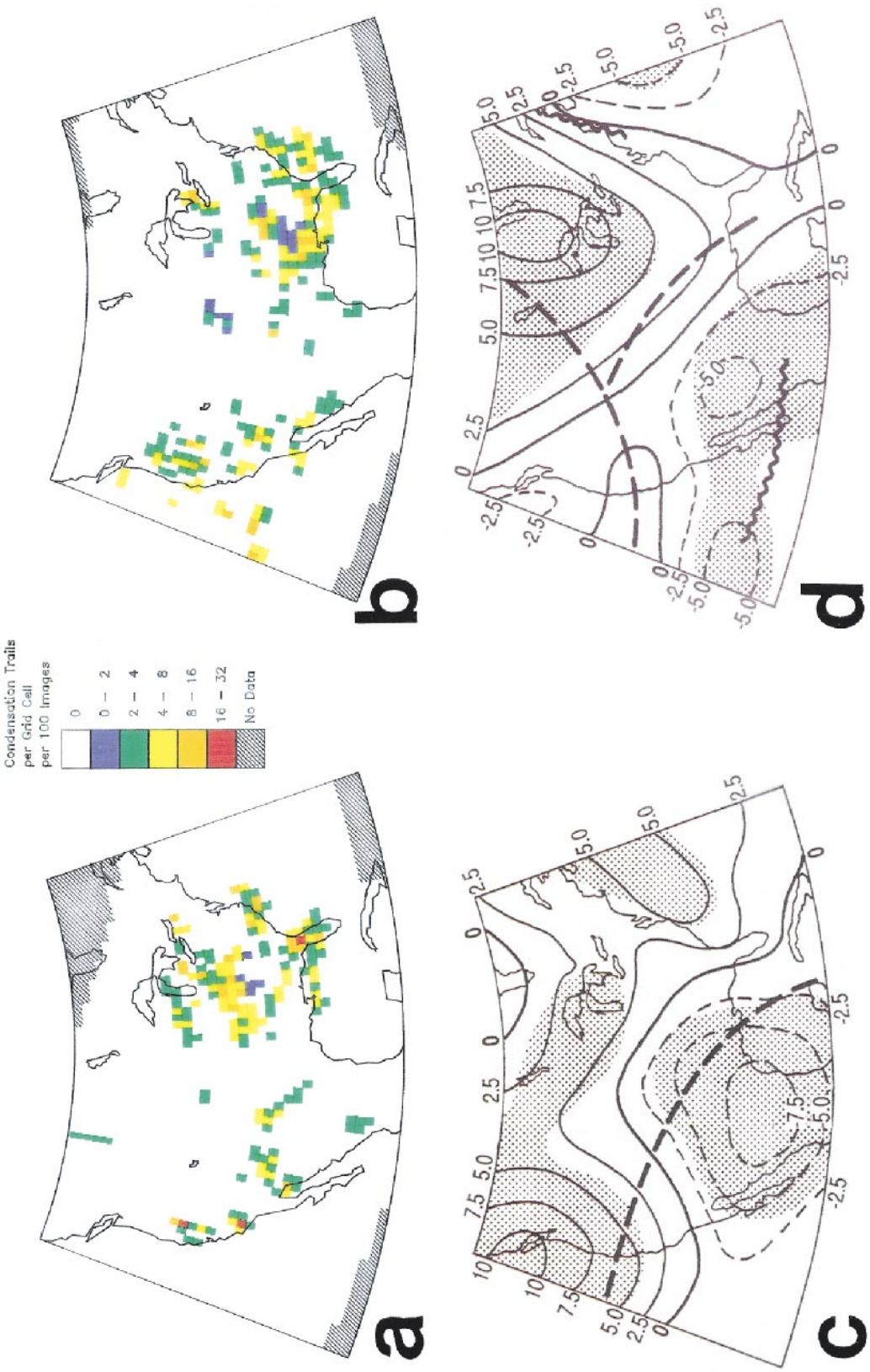


FIG. 10. Same as Fig. 8 but for (a) and (c) Jan 1978 and (b) and (d) Jan 1979.

association with the midtropospheric circulation pattern. Of the 2314 contrails identified, 2274 (98.3%) were classifiable into one of the eight circulation categories (Fig. 11a), leaving only 40 contrails (1.7%) unclassified (category 9). Contrails in the unclassified category occurred mostly in situations where reliable interpolation between consecutive daily maps was difficult. A chi-square test of the contrail frequency differences among circulation types for composites of the same midseason months was highly significant ($p < 0.001$ level), confirming the differentiation of contrails by synoptic categories. Figure 11a suggests that more contrails (78.9%) are associated with the baroclinic waves and the jet stream (categories 3–6 and 8), than with the more barotropic types (categories 1, 2, and 7; 21.1%). This result is consistent with the monthly averaged result presented in section 3b (above) and with the results of Changnon et al. (1980) and Carleton and Lamb (1986). It also follows from the association between vertical motion and moistening of the atmosphere, which is greatest in areas of enhanced horizontal temperature gradient (baroclinity), such as on the equatorward side of the jet stream. There also, the negative, or anticyclonic, shear component of the relative vorticity is accompanied by divergence in the upper troposphere (from consideration of the Simplified Vorticity Theorem). Very low contrail frequencies occur in categories 1 and 2 (closed lows and closed highs). This result is from the lack of appreciable baroclinity in the upper troposphere associated with these systems. Relatively high contrail frequencies (18.9%) occur in category 7, or zonal flow having a weak height gradient, however, which peaks in July over the study region. This result likely reflects the moistening of the upper troposphere in the summer hemisphere (e.g., Wang et al. 1996).

The day-level comparison of contrails and circulation categories confirms, for a greater number of months, the synoptic associations of contrails revealed in Carleton and Lamb (1986). It also permits examination of features only hinted at in that earlier study. For example, there is only a small difference between the contrail frequencies observed for all study months east of a trough (category 6; 15.6%) and those located east of a ridge (category 5; 17.0%). This result is somewhat surprising in view of the suggested strong dependence of contrail formation on temperature (Appleman 1953) and the apparent differences in temperature advection, relative humidity, and sign of the vertical motion between categories 6 (warm, moist, and uplift, respectively) and 5 (cold, dry, and subsidence, respectively) (e.g., Peters 1993). This result also differs from aircraft-level observations (Changnon et al. 1980) that suggested a higher percentage of contrails associated with cold advection on the west side of a trough. The aircraft observations probably were biased by the ability to see contrails better in clear air at flight level (behind a trough) than in the overrunning warm air ahead of a midlatitude cyclone, however. The near equivalence reported here is consistent with the earlier satellite-based pilot study by Carleton and Lamb (1986). In addition, the associations of contrails with specific portions of the tropospheric waves revealed by the day-level analysis (Fig. 11a) were obscured by the monthly time averaging of contrails and the atmospheric circulation in section 3b (above), especially the wind speed anomalies. The somewhat inconclusive results of that section are illuminated further by day-level comparisons of contrails and their categories of associated natural cloudiness (below).

### *d. Contrail associations with natural clouds*

Information on the natural cloud cover associated with contrails was extracted from the DMSP DR images for each contrail observation and is presented in Fig. 11b. This extraction permitted further inferences to be made about the large-scale physical processes that promot contrail formation (Jasperson et al. 1985; Liou 1986). After Carleton and Lamb (1986), seven categories of satellite-observed cloud types were used: 1) jet stream cirrus, 2) frontal cloud band of cirrostratus and altostratus/nimbostratus (jet stream cirrus also may be present), 3) cirrus cloud shield associated with a warm front or east side of a depression, 4) patchy cirrus apparently not related to categories 1–3, 5) low clouds (no natural high clouds present), 6) clear air (no clouds), 7) cirrus associated with thunderstorm blow-off, and 8) unclassified. ''No (high) clouds'' (categories 5 and 6) means an absence of clouds within an approximately 100-km radius of a contrail. Cloud categories 1–3 are most closely associated with the baroclinic circulation pattern types 3–6 and 8 (Fig. 11a). A chi-square test performed on the differences among total frequencies of contrails in each cloud category, weighted by the number of images but with categories 5 (low cloud) and 6 (clear) combined to help to fulfill the test requirements, is highly significant ($p < 0.001$). As in the classification of contrails by synoptic categories, this analysis supports the association of contrails with specific classes of natural cloudiness: notably, with cirrus (e.g., Gayet et al. 1996).

Of the 2314 contrails identified for the 11 study months, 2177 (94%) were assigned to one of the cloud categories. The remaining 6% of contrails (unclassified, category 8) did not fall clearly into one of the categories. Figure 11b shows that virtually all contrails identified (95.5%) were associated with some kind of natural high cloudiness (categories 1–4), with slightly more than half of these in the ''baroclinic'' categories (1–3). Accordingly, these cirrus baroclinic categories are at a maximum in January (categories 1 and 3), and April (category 2), and a minimum in July. Category 4 (patchy cirrus) alone accounts for nearly half (46.2%) of all classified contrails and was the modal category in 3 of the 4 months (April, July, and October). Its distribution is more even throughout the year, exhibiting a relative

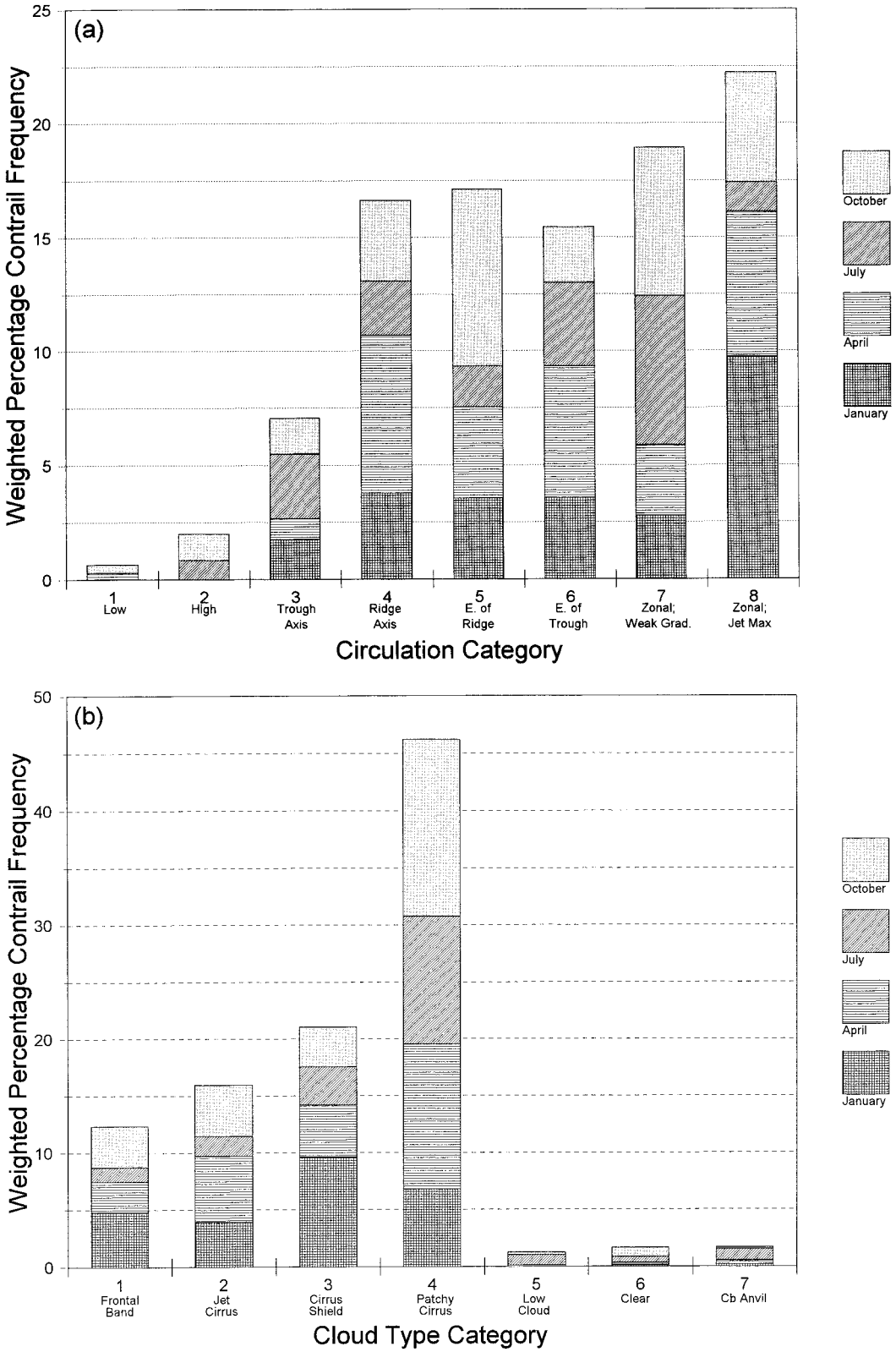


FIG. 11. Percentage frequencies of contrails in eight synoptic circulation categories, weighted according to the occurrence frequencies of (a) each synoptic type, and (b) in seven cloud groups (Cb is cumulonimbus), normalized to the number of images analyzed.

TABLE 3. Location and date of DMSP satellite imagery and rawinsonde data used in contrail case event studies for the areas delineated in Fig. 2. The circulation and cloud types are as defined in sections 3c,d and Fig. 11. The asterisk indicates image on which contrails were observed. Here $t_0$ is the rawinsonde sounding nearest in time to the contrail outbreak.

| Case study | Images analyzed | | | Nearest rawinsonde stations | Cloud type | Circulation type | Time of $t_0$ sounding |
|---|---|---|---|---|---|---|---|
| | Date | Time (UTC) | Location | | | | |
| 1 | 18 Jan 1978<br>19 Jan 1978<br>20 Jan 1978<br>21 Jan 1978 | 0253<br>0236*<br>0218<br>0201 | Eastern Midwest | Salem, IL, and Dayton, OH | 3 | 6 | 0000 UTC 19 Jan 1978 |
| 2 | 14 Jan 1978<br>16 Jan 1978<br>17 Jan 1978 | 0220<br>1538*<br>1702 | North-central Florida | Tampa, FL, and Waycross, GA | 2 | 5 | 1200 UTC 16 Jan 1978 |
| 3 | 27 Apr 1977<br>28 Apr 1977<br>29 Apr 1977<br>30 Apr 1977 | 0737<br>0720<br>0702*<br>0645 | Southern California | Vandenberg Air Force Base, CA, Point Mugu, CA, and Desert Rock, NV | 2 | 6 | 1200 UTC 29 Apr 1977 |

minimum in winter when the baroclinic types (1–3) dominate.

Figure 11b also provides insights into the annual variation in contrail frequencies shown in Fig. 5 and is consistent with the seasonal change in natural cirrus generation processes over the extratropics suggested by Jasperson et al. (1985) and Liou (1986). In particular, the dominant cloud category associated with contrails in January (category 3, cirrus cloud shields associated with warm fronts) is consistent with the annual cycle of cyclonic activity over middle latitudes and the existence of large regions of supersaturated air in the upper troposphere downstream of baroclinic disturbances (Ludlum 1980). Similarly, the percentage frequency of contrails associated with thunderstorms (category 7) peaks in midsummer (July; e.g., Jasperson et al. 1985), when the contrail association with jet-stream cirrus is at a minimum because of the northward migration of the polar-front jet stream to latitudes largely outside the study area. The dominant association of contrails with natural cirrus clouds (Fig. 11b) also helps to explain the near equivalence of contrails observed near or within an upper ridge (synoptic types 5–7, Fig. 11a): patchy cirrus (cloud category 4) typically occurs there. The near opposition in sign of the upper-tropospheric temperature advection that is implied for contrails forming in association with synoptic categories 5 (east of a ridge) and 6 (east of a trough) requires clarification, however, which is undertaken on a case study basis, below.

## 4. Case event analyses

### *a. Methodology*

Rawinsonde data on temperature and wind for three pronounced contrail outbreak events that occurred during the study months were analyzed. The criteria for defining any outbreak of contrails on the DR imagery were as follows.

1) At least eight contrails in an area of approximately 160 000 km$^2$ (i.e., 1 contrail per 20 000 km$^2$). Contrail outbreaks from commercial jets have been observed at these scales (e.g., Minnis et al. 1998). This criterion also helped to ensure that the conditions producing contrails were not random or highly localized.
2) The above contrails were within a 50-km radius of a rawinsonde station for which upper-tropospheric temperature and wind data were available for the outbreak period. This criterion ensured that the rawinsonde data were representative of conditions in the area of contrails.
3) An absence of contrails in the same area on the DR image(s) for the following day. This criterion facilitated comparisons of the rawinsonde data at the same stations for noncontrail days.

Ten contrail outbreaks in the study months satisfied the above criteria. Three representative cases occurring in very different parts of the United States (Fig. 2, Table 3) are analyzed here for the associated thermodynamic characteristics, using rawinsonde data at standard and significant pressure levels. These data were obtained from The Northern Hemisphere Data Tabulations (available on microfilm from the National Climatic Data Center, Asheville, North Carolina). Vertical temperature profiles were constructed for each contrail outbreak for the sounding closest in time to the image on which contrails were identified ($t_0$) and also for soundings 24 and 48 h prior to $t_0$ (i.e., $t_0 - 24$ and $t_0 - 48$) and following $t_0$ (i.e., $t_0 + 24$ and $t_0 + 48$). Dewpoint temperature profiles could not be included in this analysis, because the relative humidity (RH) values from which they were derived were not reported above the 400-hPa level, at the highest, because of well-documented measurement uncertainties there (e.g., Elliott and Gaffen 1991; Garand et al. 1992). Moreover, an assessment of the National Centers for Environmental Prediction–National Center for Atmospheric Research 40-Yr Reanalysis dataset (Kalnay et al. 1996) rates the humidity val-

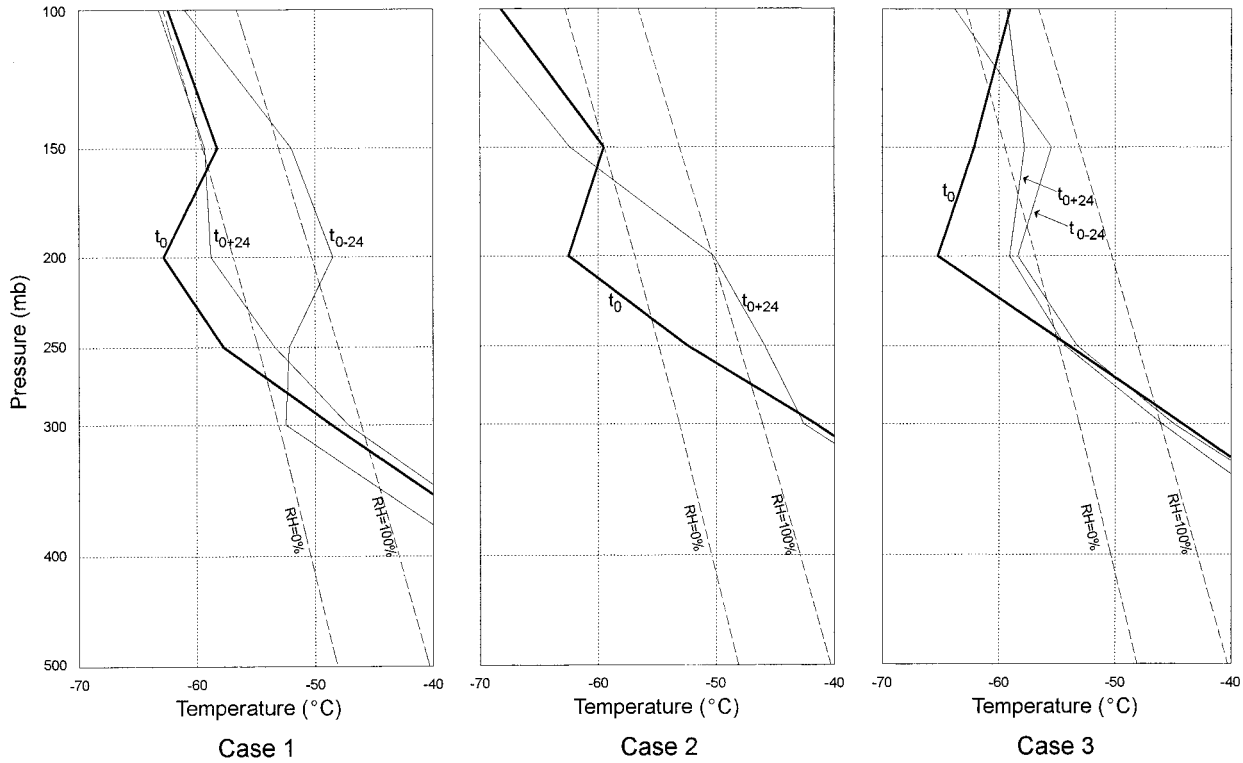


FIG. 12. Upper-tropospheric and lower-stratospheric temperature profiles for 48-h periods ($t_0 - 24$, $t_0$, $t_0 + 24$) spanning the three contrail outbreak cases (numbered; refer to Fig. 2 and Tables 3 and 4) discussed in section 4b. The data are given for the standard pressure levels only, because of averaging across rawinsonde stations for each of the three cases. The two RH lines (i.e., 100% and 0%) bound the occurrence of contrails determined experimentally to be a function of ambient pressure, temperature, and RH (from Pilié and Jiusto 1958, their Fig. 4). They pertain to the production of 0.004 g $m^{-3}$ of liquid water in a water-saturated (the 100% RH line) and a perfectly dry (the 0% RH line) environment. In each graph, contrails are never expected (always expected) when the ambient temperature at a given pressure lies to the right (left) of the RH = 100% (RH = 0%) line. The frequency of contrail formation within the 0%–100% RH range depends upon the actual RH of the air.

TABLE 4. Mean tropopause height, pressure and temperature for case event studies documented in Fig. 2 and Table 3.

| Case study | $t_0 - 48$ | $t_0 - 24$ | $t_0$ | $t_0 + 24$ | $t_0 + 48$ |
|---|---|---|---|---|---|
| | Mean tropopause height (gpm) | | | | |
| 1 | | 9524 | 11885 | 11052 | 10038 |
| 2 | 9705 | | 12447 | 10116 | |
| 3 | 11696 | 12072 | 12319 | 12306 | |
| | Mean tropopause pressure (hPa) | | | | |
| 1 | | 308 | 230 | 255 | 289 |
| 2 | 301 | | 214 | 286 | |
| 3 | 235 | 224 | 217 | 218 | |
| | Mean tropopause temperature (°C) | | | | |
| 1 | | −55.0 | −63.7 | −60.8 | −52.7 |
| 2 | −44.2 | | −65.0 | −47.0 | |
| 3 | −58.0 | −58.9 | −67.9 | −61.1 | |

ues contained therein as "reliability class B." Data in this class contain some observations, but there is also a "very strong influence" of the model on the analysis values. Kalnay et al. (1996) urge caution in using these data. Accordingly, we decided that analyzing the upper-tropospheric humidity data (where available) in our study was not appropriate. A lack of reliable humidity data also was noted to be a limitation in the recent contrail study by Poellot et al. (1999).

Tropopause heights and temperatures were determined by inspection of complete sounding information (i.e., the temperature and wind data at both the standard and significant levels). Because each contrail outbreak area extended over two or three adjacent rawinsonde stations, the sounding data were averaged over these stations after confirming that no major differences existed between temperature profiles at a particular time. The station-averaged results for the standard levels are plotted in Fig. 12; those for all available levels (i.e., the standard plus significant and tropopause levels) are given in Table 4. Although generally comparable, small differences in the temperature average values for the three cases are evident between Table 4 and Fig. 12.

They reflect the lower vertical resolution of the graphical (Fig. 12) versus tabular (Table 4) data.

The upper-tropospheric horizontal temperature advection for the above three contrail outbreak events was examined for the 500–300-, 300–200-, 300–250-, and 250–200-hPa layers. These computations were performed for individual rawinsonde stations using the following standard steps (e.g., McIntosh and Thom 1969, chapter 6.5): 1) determine the layer-mean thermal wind vector $\mathbf{V}_T$ from the difference between the geostrophic wind vectors at the bottom and top of an isobaric layer, 2) derive the horizontal gradient of the mean virtual temperature associated with $\mathbf{V}_T$, and 3) compute the instantaneous (local) horizontal temperature advection from the mean temperature gradient and the component of the layer-mean geostrophic wind $\mathbf{V}_N$ normal to $\mathbf{V}_T$. The layer mean virtual temperature is assumed to be equivalent to its mean ambient temperature and is calculated as the arithmetic mean of the temperatures at two levels except for layers having one or more standard levels between the upper and lower boundaries. In those cases, the mean temperature was calculated iteratively using the equal-area method (Wallace and Hobbs 1977, p. 58). Thicknesses were calculated using the hypsometric equation.

### *b. Contrail layer-temperature and tropopause associations*

All three case studies provide strong evidence that contrails occurred when and where the tropopause was colder and also higher at $t_0$ (contrail time) than at 24 and 48 h prior to or following $t_0$ (Table 4). These tropopause characteristics are associated typically with ridges in the upper-tropospheric geopotential height field (e.g., Wallace and Hobbs 1977, their Fig. 9.13; Carlson 1991, chapter 10.5). The three-case contrail mean tropopause temperature (height) of −64.3°C (12.5 km) was 8°C colder (1.3 km higher) than for the immediately preceding and following soundings ($t_0 - 24$, $t_0 - 48$, $t_0 + 24$, and $t_0 + 48$) without contrails (−56.3°C, 11.2 km). The lower, warmer tropopause of the noncontrail soundings occurs below the typical midlatitude cruising altitude of long-distance commercial jet aircraft, especially for the colder-season months considered here (e.g., Hoinka et al. 1993: their Fig. 11). This cruising altitude is generally located at about 11.5 km, or in the 250–200-hPa layer (Beckwith 1972; Machta and Telegadas 1974), which is consistent with the current observation of contrails when the tropopause is higher near 200 hPa (Fig. 12). Moreover, the 250–200-hPa temperatures are colder at $t_0$ than at those other times. The drier conditions of the lower stratosphere would be less favorable to persisting contrails than those of the upper troposphere.

Although the number of analyzed cases is too small to permit definitive conclusions regarding the statistical significance of the results, the rawinsonde data reveal that generally large changes in tropopause temperature/height and upper-tropospheric temperatures accompany the outbreaks of contrails, as revealed by the satellite analysis. The upper-tropospheric temperature profiles for these case events also largely are consistent with early key theoretical (Appleman 1953) and laboratory (Pilié and Jiusto 1958) investigations. Pilié and Jiusto modified Appleman's nomogram describing the critical temperature and RH values necessary for contrail formation (the 0% and 100% RH curves in Fig. 12). This modification was necessitated by discrepancies in the frequencies with which contrails were observed to occur in project CLOUD TRAIL (Air Weather Service 1956) and those predicted to occur theoretically. Pilié and Jiusto (1958) attributed this difference mostly to the ratio describing the change in mixing ratio in the aircraft wake to the change in wake temperature. This ratio is a function of the aircraft fuel, and was given as 0.0336 g $kg^{-1}$ $K^{-1}$ by Appleman (1953) but was changed to a more representative value of 0.0295 g $kg^{-1}$ $K^{-1}$ by Pilié and Jiusto (1958). Subsequent improvements in jet engine performance also have modified these ''contrail-factor'' values (Schrader 1997). In Fig. 12, contrail formation (assumed to occur at a water concentration of 0.004 g $m^{-3}$) *outside* of the region bounded by the 0% and 100% RH lines is determined by the ambient temperature. Because the atmosphere is rarely supersaturated with respect to water, contrails should rarely form to the right of the 100% line (Appleman 1953), however. To the left of the 0% line, temperatures will be sufficiently low for contrails always to form, even in dry air. Contrail formation at intermediate ambient temperatures (i.e., *within* the region bounded by the 0% and 100% RH lines on Fig. 12) depends upon whether the measured RH exceeds the required value (Appleman 1953; Pilié and Jiusto 1958). Subsequent empirical studies (e.g., Hanson and Hanson 1995) confirm that contrails have a very low probability of forming to the right of the RH = 100% line, but the probability of contrail formation to the left of the RH = 0 percent line, while high, is somewhat less than ''always.'' This fact is because measured RH values of 0% at these altitudes require a temperature much lower than what is observed. Although contrail formation also depends on engine type and contrail factor (Peters 1993; Schrader 1997), there apparently is little sensitivity to the fuel sulfur content (Busen and Schumann 1995).

In Fig. 12, the temperature data for the 250–200-hPa layer for the three contrail outbreak events tend to support the pioneering studies of Appleman (1953) and Pilié and Jiusto (1958): contrails were observed on the DR imagery at $t_0$ when temperatures in the upper troposphere were to the left of the 0% RH line. Although conditions in the upper troposphere also appear to be favorable for contrail formation at $t_0 + 24$ in case 1, at $t_0 + 24$ in case 2, and at $t_0 + 24$ and $t_0 - 24$ in case 3, contrails were not observed on the imagery at these times. For cases 1 and 3, this result likely is because of

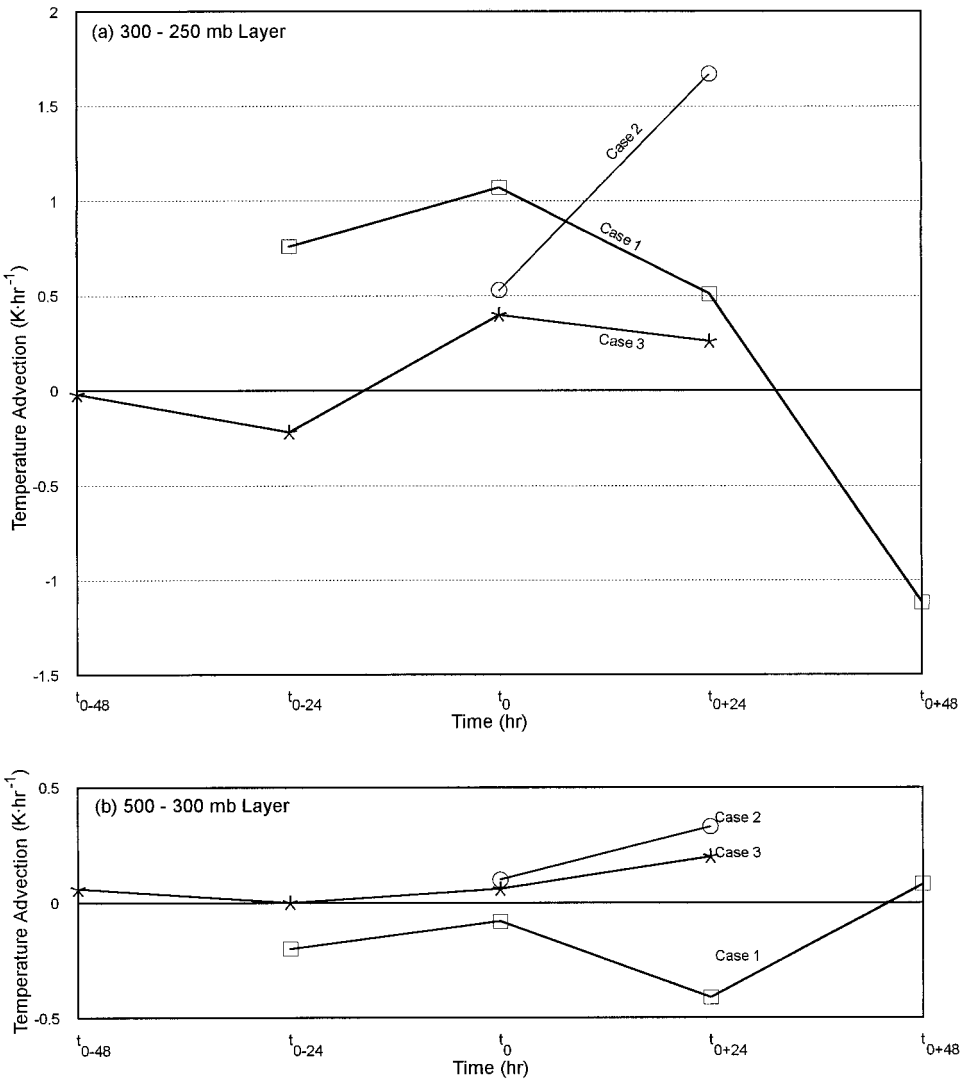


FIG. 13. Temporal variation of the horizontal advection of temperature (K $h^{-1}$) for the three contrail outbreak cases documented in Fig. 2 and Tables 3 and 4: (a) 300–250-hPa layer and (b) 500–300-hPa layer. The abscissa indicates sounding times (h) before and following the satellite-observed peak of the contrail outbreak ($t_0$).

only a thin layer of the atmosphere being ''favorable'' for contrails at times other than $t_0$, which reduces the probability that jet aircraft will occur in that layer, or that contrails so formed will persist. The absence of contrails at $t_0 + 24$ in case 2 probably is explained by the favorable temperature conditions occurring at altitudes higher than (pressure $<$ 165 hPa) the typical cruising levels of subsonic aircraft.

### *c. Temperature advection in contrail environments*

For each contrail outbreak, Fig. 13 gives the temperature advection for the layer in which contrails are most likely to occur (300–250 hPa) and for the thicker layer immediately below (500–300 hPa). No strong patterns of temperature advection are evident for the lower (500–300 hPa) layer. Warm advection of a greater magnitude is evident in the 300–250-hPa layer at $t_0$ for cases 1 and 3 and at $t_0 + 24$ for case 2 (Fig. 13), however. The patterns for cases 1 and 3 (case 2) are consistent with a location to the west (east) of an upper-air ridge at $t_0$ (e.g., Carlson 1991, chapters 4.3 and 10.5; our Table 3). The differences in magnitude of the 300–250-hPa layer-averaged temperature advection between cases are likely the result of differences in location and time of year of the contrail outbreaks (Table 3, Fig. 2). Thus, the results for the three cases are consistent with the earlier finding on a monthly timescale that contrails are about as frequent east of a trough as east of a ridge. Further insights again require information on the upper-tropospheric moisture conditions that are not available here.

## 5. Summary and discussion

A satellite-based climatic description of persistent linear jet contrails, developed for 11 midseason months in 1977–79 and covering the conterminous United States and adjacent regions, was derived from subjective interpretation of high-resolution IR images acquired by the DMSP polar orbiters. This is the first contrail investigation to cover such a large area for so many months with a fine spatial resolution (1° lat × 1° long). It avoids the observational biases of previous efforts based on ground- or flight-level data. The manual method of identifying contrails on the imagery is supported by the ''verification'' study (section 2b), which also confirms satellite observations to be superior to surface observations when cloud cover is present and on these larger spatial scales (see also Carleton and Lamb 1986; Bakan et al. 1994). The rigorous criteria used to identify contrails undoubtedly excludes less obvious and older contrails that have become sufficiently diffuse not to be differentiated reliably from natural cirrus and emphasizes contrails that are relatively ''fresh'' (cf. Mannstein et al. 1999). Detwiler and Pratt (1984) estimated the age of contrails they observed on Landsat imagery to be less than 1 h, although remnants may be recognizable from the surface for somewhat longer. The ability to observe contrail evolution using images at higher temporal frequency would, therefore, be advantageous for future studies.

Contrail variations through the study months were determined, along with their associations with the background cloudiness and the larger-scale atmospheric circulation. The major results and implications of this investigation were as follows:

1) Contrails are a widespread phenomenon over the United States and adjacent regions, being observed in virtually every region at one time or another during the study months. They most frequently are observed over the following regions: 1) the southwestern United States (especially southern California), 2) the southeastern United States (specifically, southeastern Georgia and north-central Florida); 3) the coast of British Columbia, including Vancouver Island; and 4) a large portion of the eastern part of the Midwestern United States centered over southeastern Indiana and western Kentucky. Conversely, contrails are observed infrequently in the southern and northern regions of the study area (the Gulf of Mexico and southern Canada) and the mountainous areas of the western United States. The preferred regions of contrail occurrence identified in this dataset for 1977–79 result from both high frequencies of aircraft flight and atmospheric conditions favorable for contrail formation and persistence (see also Bakan et al. 1994). Their longer-term representativeness is supported by the considerable similarity between the overall distribution in the current Fig. 4 and Sassen's (1997) map (his Fig. 2) of the amount of fuel burned by commercial and military jets during one more-recent month (May 1990).
2) Contrail frequencies are highest in the northernmost (southernmost) latitudes of the study area during July (January), whereas they peak in middle latitudes during the transition months of April and October. This variation coincides with the annual variation in latitudinal extent and intensity of the westerly circulation: farthest equatorward (poleward), on average, in the winter (summer). There is also an annual change in contrail frequencies for the entire study area. The highest frequencies occur during the transition months, and the lowest frequencies are in summer, which suggests the role of strong temperature gradients (baroclinity) in ultimately promoting contrail formation at the altitudes typically flown by jet aircraft.
3) Virtually all contrails are associated with naturally occurring high-level cloudiness. The most frequent association is with patchy cirrus having no obvious direct relationship to organized cyclonic or convective systems. Although the midseason and individual mean monthly distributions of contrails (Figs. 6 and 7) are in general agreement with shorter-term surface and aircraft-based studies of contrails (Changnon et al. 1980; Wendland and Semonin 1982; Minnis et al. 1997), our finding of a possible contrail maximum for the United States in autumn as well as in spring is particularly interesting in light of the cirrus cloud climatic description developed by Woodbury and McCormick (1986). That study showed a minimum in the cirrus (''high cloud'') fraction over the United States during autumn. The coincidence of a contrail maximum and natural cirrus minimum would increase the potential effect of contrails on the surface climate during the autumn. On both continental and regional scales, some of the strongest increases (decreases) in surface-reported cloudiness (percent possible sunshine and global radiation) have occurred in the autumn season (Changnon 1981; Angell 1990; Petersen et al. 1995). For the Midwest in particular, the autumn season has seen some of the strongest upward trends in ''moderated'' temperatures (i.e., reduced diurnal temperature range) consistent with increases in high cloudiness (Changnon 1981; Travis and Changnon 1997; Allard 1997).
4) Examination of averaged circulation anomalies for the study months suggests that increased regional frequencies of contrails on that timescale may be associated with significant departures of upper-tropospheric height and/or vector wind speed from the long-term monthly means. These circulation anomalies are accompanied by large spatial variations in vorticity and wind shear, again implying the importance of baroclinity, at least on timescales greater than about 30 min (cf. Chlond 1998).
5) Comparisons of daily midtropospheric circulation patterns with contrail occurrences confirm their syn-

optic associations, most frequently with baroclinic phenomena (wave cyclones, jet streams). Contrails also occur in association with upper-tropospheric ridges, although there is little difference in the frequencies of contrails on the west side of a ridge as compared with the east side of a ridge. An analysis of the time-dependent temperature characteristics of the atmospheric layer in which contrails occur most frequently, for three ''representative'' outbreaks, confirms a contrail association with upper ridgelines. This is evident from an increase in the height, and associated cooling, of the tropopause level, which increases the opportunity for aircraft to make contrails in the upper troposphere. Within an upper trough, however, jet aircraft are less likely to make contrails, because they would be flying in the drier low stratosphere. The three cases also strongly support early pioneering studies on contrail prediction: contrails were observed on the imagery only at times (i.e., $t_0$) when the upper troposphere was very cold through a layer sufficiently deep so as to maximize the opportunities for jet aircraft to make contrails. Examination of the associated temperature advection reveals, in two cases, that the warm advection west of the upper ridgeline peaked at around the time of the contrail outbreak. In the other case, however, warm advection increased through at least $t_0 + 24$ h, consistent with a contrail location east of the ridge at $t_0$. Further clarification of these results requires that more cases be examined and should include information on the upper-tropospheric moisture. In this respect, Travis et al. (1997) demonstrate, using information from the Geostationary Operational Environmental Satellite, that the column-integrated water vapor for 700–100-hPa is at least as important as the layer-averaged temperature in predicting contrail formation. Moreover, a numerical modeling study of the physical processes controlling contrail evolution (Chlond 1998) indicates that humidity, temperature, and also the static stability of the environment determine contrail growth. Along with other workers (e.g., Peters 1993; Poellot et al. 1999), this author calls for high-quality observations of humidity in the upper troposphere.

The research reported here is providing the basis for an ongoing assessment of the radiative and climatic effects of contrails for the regions of the United States that have been shown to be highly favored for contrail formation (e.g., Travis 1994, 1996a,b; Travis et al. 1997; Allard 1997). These studies are a necessary prerequisite to determining more exactly the role of contrail cirrus in recent climate changes observed at regional scales over the United States.

*Acknowledgments.* This research was supported, in part, by NOAA Grant COMM-NA89RA-H-09086 to the Illinois State Water Survey, by the ARM Program of the U.S. Department of Energy through Battelle PNL Contract 144880-A-Q1 to the Cooperative Institute for Mesoscale Meteorological Studies (CIMMS) at the University of Oklahoma, and by a travel grant from the Indiana University (IU) Center for Transportation Research. We appreciate the time and assistance of the staff at the National Snow and Ice Data Center, CIRES, University of Colorado, Boulder, who made available the DMSP imagery. David L. Arnold (IU) assisted DJT in the surface observations of contrails at Bloomington, Indiana. We are grateful to the anonymous reviewers for their helpful and insightful comments on the original submitted manuscript.

## REFERENCES

Ackerman, A. S., O. W. Toon, and P. V. Hobbs, 1995: Numerical modeling of ship tracks produced by injections of cloud condensation nuclei into marine stratiform clouds. *J. Geophys. Res.,* **100,** 7121–7133.

Air Weather Service, 1956: Forecasting of aircraft condensation trails. Air Weather Service Manual 105-100 (REV), Air Weather Service, Scott AFB, IL, 17pp.

Allard, J., 1997: The climatic impacts of jet airplane condensation trails (contrails) in the Northeast U.S. M.S. thesis, Dept. of Geography, The Pennsylvania State University, 152 pp. [Available from Dept. of Geography, The Pennsylvania State University, University Park, PA 16802.]

Angell, J. K., 1990: Variation in United States cloudiness and sunshine duration between 1950 and the drought year of 1988. *J. Climate,* **3,** 296–308.

——, J. Korshover, and G. F. Cotton, 1984: Variation in United States cloudiness and sunshine, 1950–82. *J. Climate Appl. Meteor.,* **23,** 752–761.

Appleman, H., 1953: The formation of exhaust condensation trails by jet aircraft. *Bull. Amer. Meteor. Soc.,* **34,** 14–20.

Arking, A., 1991: The radiative effects of clouds and their impact on climate. *Bull. Amer. Meteor. Soc.,* **72,** 795–813.

Bakan, S., M. Betancor, V. Gayler, and H. Grassl, 1994: Contrail frequency over Europe from NOAA-satellite images. *Ann. Geophys.,* **12,** 962–968.

Beckwith, W. B., 1972: Future patterns of aircraft operations and fuel burnouts with remarks on contrail formation over the United States. Preprints, *Int. Conf. on Aerospace and Aeronautical Meteorology,* Washington, DC, Amer. Meteor. Soc., 422–426.

Boin, M., and L. Levkov, 1994: A numerical study of contrail development. *Ann. Geophys.,* **12,** 969–978.

Brogniez, G., J. C. Buriez, V. Giraud, F. Parol, and C. Vanbauce, 1995: Determination of effective emittance and a radiatively equivalent microphysical model of cirrus from ground-based and satellite observations during the International Cirrus Experiment: The 18 October 1989 case study. *Mon. Wea. Rev.,* **123,** 1025–1036.

Bryson, R. A., and W. M. Wendland, 1975: Climatic effects of atmospheric pollution. *The Changing Global Environment,* S. F. Singer, Ed., Reidel, 139–147.

Busen, R., and U. Schumann, 1995: Visible contrail formation from fuels with different sulfur contents. *Geophys. Res. Lett.,* **22,** 1357–1360.

Cairns, B., 1993: Inter and intra-annual cloud variations from satellite-based climatologies. Preprints, *Fourth Symp. on Global Change Studies,* Anaheim, CA, Amer. Meteor. Soc., 245–248.

Carleton, A. M., 1988: Meridional transport of eddy sensible heat in winters marked by extremes of the North Atlantic Oscillation, 1948/49–1979/80. *J. Climate,* **1,** 212–223.

——, and P. J. Lamb, 1986: Jet contrails and cirrus cloud: A feasibility

study employing high-resolution satellite imagery. *Bull. Amer. Meteor. Soc.,* **67,** 301–309.
Carlson, T. N., 1991: *Mid-Latitude Weather Systems.* HarperCollins Academic, 507 pp.
Cerveny, R. S., and R. C. Balling Jr., 1990: Inhomogeneities in the long-term United States' sunshine record. *J. Climate,* **3,** 1045–1048.
Changnon, S. A., 1981: Midwestern cloud, sunshine and temperature trends since 1901: Possible evidence of jet contrail effects. *J. Appl. Meteor.,* **20,** 496–508.
——, R. G. Semonin, and W. M. Wendland, 1980: Effect of contrail cirrus on surface weather conditions in the Midwest: Phase I. Final Report of NSF Grant ATM 78-09568, Illinois State Water Survey, Champaign, 141 pp. [Available from Atmospheric Sciences Division, Illinois State Water Survey, 2204 Griffith Dr., Champaign, IL 61820-7495.]
Chlond, A., 1998: Large-eddy simulation of contrails. *J. Atmos. Sci.,* **55,** 796–819.
Coakley, J. A., Jr., R. L. Bernstein, and P. A. Durkee, 1987: Effect of ship-stack effluents on cloud reflectivity. *Science,* **237,** 1020–1022.
Croke, M. S., R. D. Cess, and S. Hameed, 1999: Regional cloud cover change associated with global climate change: Case studies for three regions of the United States. *J. Climate,* **12,** 2128–2134.
DeGrand, J. Q., 1991: A satellite-derived mid-season climatology of jet condensation trails: April 1977–October 1979. M.A. thesis, Dept. of Geography, Indiana University, 117 pp. [Available from Dept. of Geography, Indiana University, Bloomington, IN 47405.]
Detwiler, A., 1983: Effects of artificial and natural cirrus clouds on temperatures near the ground. *J. Wea. Modif.,* **15,** 45–55.
——, and R. Pratt, 1984: Clear-air seeding: Opportunities and strategies. *J. Wea. Modif.,* **16,** 46–60.
Dowling, D. R., and L. F. Radke, 1990: A summary of the physical properties of cirrus clouds. *J. Appl. Meteor.,* **29,** 970–978.
Duda, D. P., J. D. Spinhirne, and W. D. Hart, 1998: Retrieval of contrail microphysical properties during SUCCESS by the split-window method. *Geophys. Res. Lett.,* **25,** 1149–1152.
Elliott, W. P., and D. J. Gaffen, 1991: On the utility of radiosonde humidity archives for climate studies. *Bull. Amer. Meteor. Soc.,* **72,** 1507–1520.
Engelstad, M., S. K. Sengupta, T. Lee, and R. M. Welch, 1992: Automated detection of jet contrails using the AVHRR split window. *Int. J. Remote Sens.,* **13,** 1391–1412.
Federal Aviation Administration, 1979: Current aviation statistics—air traffic activity: Enroute IFR air traffic survey, peak day—fiscal year 1977. U.S. Govt. Printing Office, Washington, DC, 53 pp.
Fett, R. W., and W. F. Mitchell, 1977: Anomalous grey shades—aircraft condensation trails. *Navy Tactical Applications Guide,* Vol. 1, *Techniques and Applications of Image Analysis,* Naval Environmental Prediction Research Facility, 35.
Fortuin, J. P. F., R. Van Dorlund, W. M. F. Wauben, and H. Kelder, 1995: Greenhouse effects of aircraft emissions as calculated by a radiative transfer model. *Ann. Geophys.,* **13,** 413–418.
Freeman, K. P., and K.-N. Liou, 1979: Climatic effects of cirrus clouds. *Advances in Geophysics,* Vol. 21, Academic Press, 231–287.
Garand, L., C. Grassotti, J. Halle, and G. L. Klein, 1992: On differences in radiosonde humidity-reporting practices and their implications for numerical weather prediction and remote sensing. *Bull. Amer. Meteor. Soc.,* **73,** 1417–1423.
Gayet, J.-F., G. Febvre, G. Brogniez, H. Chepfer, W. Renger, and P. Wendling, 1996: Microphysical and optical properties of cirrus and contrails: Cloud field study on 13 October 1989. *J. Atmos. Sci.,* **53,** 126–138.
Gothe, M. B., and H. Grassl, 1993: Satellite remote sensing of the optical depth and mean crystal size of thin cirrus and contrails. *Theor. Appl. Climatol.,* **48,** 101–113.
Grassl, H., 1990: Possible climatic effects of contrails and additional water vapour. *Air Traffic and the Environment—Background, Tendencies and Potential Global Atmospheric Effects,* U. Schumann, Ed., Springer Verlag, 124–137.
Hall, F. H., 1970: Pollution in the upper troposphere by soot from jet aircraft and its relation to cirrus clouds (abstract). *Bull. Amer. Meteor. Soc.,* **51,** 101.
Hanson, H. M., and D. M. Hanson, 1995: A reexamination of the formation of exhaust condensation trails by jet aircraft. *J. Appl. Meteor.,* **34,** 2400–2405.
Harami, K., 1968: Utilization of condensation trails for weather forecasting. *J. Meteor. Res. Japan,* **20,** 55–63.
Henderson-Sellers, A., 1992: Continental cloudiness changes this century. *GeoJournal,* **27,** 255–262.
——, and K. McGuffie, 1989: Diagnosis of cloud amount increase from an analogue model of a warming world. *Atmosfera,* **2,** 67–101.
Heymsfield, A. J., L. M. Miloshevich, C. Twohy, G. Sachse, and S. Oltmans, 1998: Upper-tropospheric relative humidity observations and implications for cirrus ice nucleation. *Geophys. Res. Lett.,* **25,** 1343–1346.
Hoinka, K. P., M. E. Reinhardt, and W. Metz, 1993: North Atlantic air traffic within the lower stratosphere: Cruising times and corresponding emissions. *J. Geophys. Res.,* **98,** 23 113–23 131.
Hudson, J. G., and Y. Xie, 1998: Cloud condensation nuclei measurements in the high troposphere and in jet aircraft exhaust. *Geophys. Res. Lett.,* **25,** 1395–1398.
Hunter, D. E., S. E. Schwartz, R. Wagener, and C. M. Benkovitz, 1993: Seasonal, latitudinal, and secular variations in temperature trend: Evidence for influence of anthropogenic sulfate. *Geophys. Res. Lett.,* **20,** 2455–2458.
Hutchison, K. D., K. R. Hardy, and B. C. Gao, 1995: Improved detection of optically thin cirrus clouds in nighttime multispectral meteorological satellite imagery using total integrated water vapor information. *J. Appl. Meteor.,* **34,** 1161–1168.
Jacobs, J. D., 1971: Aircraft contrail effects on the surface radiation budget in an Arctic region. *Bull. Amer. Meteor. Soc.,* **52,** 1101–1102.
Jasperson, W. H., G. D. Nastrom, R. E. Davis, and J. D. Holdeman, 1985: Variability of cloudiness at airline cruise altitudes from GASP measurements. *J. Climate Appl. Meteor.,* **24,** 74–82.
Jensen, E. J., A. S. Ackerman, D. E. Stevens, O. B. Toon, and P. Minnis, 1998: Spreading and growth of contrails in a sheared environment. *J. Geophys. Res.,* **103,** 31 557–31 567.
Joseph, J. H., Z. Levin, Y. Mekler, G. Ohring, and J. Otterman, 1975: Study of contrails observed from the *ERTS I* satellite imagery. *J. Geophys. Res.,* **80,** 366–372.
Kaiser, D. P., and V. N. Razuvaev, 1995: Cloud cover and type over the former USSR, 1936–83; trends derived from the RIHMI-WDC 223-station 6- and 3-hourly meteorological database. *Proc. 6th Int. Conf. on Statistical Climatology,* Galway, Ireland, Amer. Meteor. Soc., 419–422.
Kalnay, E., and Coauthors, 1996: The NCEP/NCAR 40-Year Reanalysis Project. *Bull. Amer. Meteor. Soc.,* **77,** 437–471.
Karl, T. R., and P. M. Steurer, 1990: Increased cloudiness in the United States during the first half of the twentieth century: Fact or fiction? *Geophys. Res. Lett.,* **17,** 1925–1928.
——, R. W. Knight, D. R. Easterling, and R. G. Quayle, 1996: Indices of climate change for the United States. *Bull. Amer. Meteor. Soc.,* **77,** 279–292.
Khvorostyanov, V., and K. Sassen, 1998: Cloud model simulation of a contrail case study: Surface cooling against upper tropospheric warming. *Geophys. Res. Lett.,* **25,** 2145–2148.
Knollenberg, R. G., 1972: Measurements of the growth of the ice budget in a persisting contrail. *J. Atmos. Sci.,* **29,** 1367–1374.
Kuhn, P. M., 1970: Airborne observations of contrail effects on the thermal radiation budget. *J. Atmos. Sci.,* **27,** 937–942.
Kuo, K. S., R. M. Welch, and S. K. Sengupta, 1988: Structural and textural characteristics of cirrus clouds observed using high spatial resolution LANDSAT imagery. *J. Appl. Meteor.,* **27,** 1242–1260.

Lawrence, M. G., 1993: An empirical analysis of the strength of the phytoplankton–dimethylsulfide–cloud–climate feedback cycle. *J. Geophys. Res.,* **98,** 20 663–20 673.

Lee, J. E., and S. D. Johnson, 1985: Expectancy of cloudless photographic days in the contiguous United States. *Photogramm. Eng. Remote Sens.,* **51,** 1883–1891.

Lee, T. F., 1989: Jet contrail identification using the AVHRR infrared split window. *J. Appl. Meteor.,* **28,** 993–995.

Liou, K.-N., 1986: Influence of cirrus clouds on weather and climate processes. *Mon. Wea. Rev.,* **114,** 1167–1199.

——, S. C. Ou, and G. Koenig, 1990: An investigation on the climatic effect of contrail cirrus. *Air Traffic and the Environment—Background, Tendencies and Potential Global Atmospheric Effects,* U. Schumann, Ed., Springer Verlag, 154–169.

——, P. Yang, Y. Takano, K. Sassen, T. Charlock, and W. Arnott, 1998: On the radiative properties of contrail cirrus. *Geophys. Res. Lett.,* **25,** 1161–1164.

Ludlum, F. H., 1980: *Clouds and Storms.* The Pennsylvania State University Press, 405 pp.

Machta, L., and T. Carpenter, 1971: Trends in high cloudiness at Denver and Salt Lake City. *Man's Impact on the Environment,* W. H. Mathews, W. W. Kellogg, and G. D. Robinson, Eds., The MIT Press, 410–415.

——, and K. Telegadas, 1974: Inadvertent large-scale weather modification. *Weather and Climate Modification,* W. N. Hess, Ed., John Wiley and Sons, 687–725.

Manabe, S., 1975: Cloudiness and the radiative convective equilibrium. *The Changing Global Environment,* S. F. Singer, Ed., Reidel, 175–176.

Mannstein, H., R. Meyer, and P. Wendling, 1999: Operational detection of contrails from NOAA-AVHRR data. *Int. J. Remote Sens.,* **20,** 1641–1660.

Mazin, I. P., S. N. Burkovskaya, and E. T. Ivanova, 1993: On the climatology of upper-level clouds. *J. Climate,* **6,** 1812–1821.

McIntosh, D. H., and A. S. Thom, 1969: *Essentials of Meteorology.* Wykeham Publications, 238 pp.

Mims, F. M., and D. J. Travis, 1997: Aircraft contrails reduce solar irradiance. *Eos, Trans. Amer. Geophys. Union,* **78,** 448.

Minnis, P., J. K. Ayers, and S. P. Weaver, 1997: Surface-based observations of contrail occurrence frequency over the U.S., April 1993–April 1994. NASA Ref. Publ. 1404, NASA Langley Research Center, Hampton, VA, 12 pp.

——, D. F. Young, D. P. Garber, L. Nguyen, W. L Smith Jr., and R. Palikonda, 1998: Transformation of contrails into cirrus during SUCCESS. *Geophys. Res. Lett.,* **25,** 1157–1160.

Molnar, G., 1993: Greenhouse sensitivity to tropical water vapor distribution and cirrus property changes. Preprints, *Fourth Symp. on Global Change Studies,* Anaheim, CA, Amer. Meteor. Soc., 104–111.

Namias, J., and P. F. Clapp, 1951: Observational studies of general circulation patterns. *Compendium of Meteorology,* T. F. Malone, Ed., Amer. Meteor. Soc., 551–567.

NASA/NOAA/UKDOE/UNEP/WMO, 1991: *Scientific Assessment of Ozone Depletion: 1991 Global Ozone Research and Monitoring Project–Report No. 25.* WMO, 295 pp.

Nicodemus, M. L., and J. D. McQuigg, 1969: A simulation model for studying possible modification of surface temperature. *J. Appl. Meteor.,* **8,** 199–204.

NMC, 1990: *NMC Grid Point Data Set.* Version 2, Dept. of Atmos. Sci., University of Washington, and Data Support Section, NCAR, CD-ROM.

Parol, F., J. C. Buriez, G. Brogniez, and Y. Fouquart, 1991: Information content of AVHRR channels 4 and 5 with respect to the effective radius of cirrus cloud particles. *J. Appl. Meteor.,* **30,** 973–984.

Parungo, F., J. F. Boatman, H. Sievering, S. W. Wilkison, and B. B. Hicks, 1994: Trends in global marine cloudiness and anthropogenic sulfur. *J. Climate,* **7,** 434–440.

Peixoto, J. P., and A. H. Oort, 1996: The climatology of relative humidity in the atmosphere. *J. Climate,* **9,** 3443–3463.

Peters, J. L., 1993: New techniques for contrail forecasting. Air Weather Service AWS/TR-93/001, AD-A269686, Air Weather Service, Scott Air Force Base, IL, 31 pp.

Petersen, M. S., P. J. Lamb, and K. E. Kunkel, 1995: Implementation of a semiphysical model for examining solar radiation in the Midwest. *J. Appl. Meteor.,* **34,** 1905–1915.

Pilié, R. J., and J. E. Jiusto, 1958: A laboratory study of contrails. *J. Meteor.,* **15,** 149–154.

Plantico, M. S., T. R. Karl, G. Kukla, and J. Gavin, 1990: Is recent climate change across the United States related to rising levels of anthropogenic greenhouse gases? *J. Geophys. Res.,* **95,** 16 617–16 637.

Platnick, S., and S. Twomey, 1994: Determining the susceptibility of cloud albedo to changes in droplet concentration with the Advanced Very High Resolution Radiometer. *J. Appl. Meteor.,* **33,** 334–347.

Platt, C. M. R., 1989: The role of cloud microphysics in high-cloud feedback effects on climate change. *Nature,* **341,** 428–429.

Poellot, M. R., W. P. Arnott, and J. Hallett, 1999: In situ observations of contrail microphysics and implications for their radiative impact. *J. Geophys. Res.,* **104,** 12 077–12 084.

Poetzsch-Heffter, C., Q. Liu, E. Ruprecht, and C. Simmer, 1995: Effect of cloud types on the earth radiation budget calculated with the ISCCP C1 dataset: Methodology and initial results. *J. Climate,* **8,** 829–843.

Ponater, M., S. Brinkop, R. Sausen, and U. Schumann, 1996: Simulating the global atmospheric response to aircraft water vapor emissions and contrails: A first approach using a GCM. *Ann. Geophys.,* **14,** 941–960.

Radke, L. F., J. A. Coakley, and M. D. King, 1989: Direct and remote sensing observations of the effects of ships on clouds. *Science,* **246,** 1146–1149.

Randel, D. L., T. H. Vonder Haar, M. A. Ringerud, G. L. Stephens, T. J. Greenwald, and C. L. Combs, 1996: A new global water vapor dataset. *Bull. Amer. Meteor. Soc.,* **77,** 1233–1246.

Reinking, R. F., 1968: Insolation reduction by contrails. *Weather,* **23,** 171–173.

Rind, D., P. Lonergan, and K. Shah, 1996: Climatic effect of water vapor release in the upper troposphere. *J. Geophys. Res.,* **101,** 29 395–29 405.

Sassen, K., 1991: Aircraft-produced ice particles in a highly supercooled altocumulus cloud. *J. Appl. Meteor.,* **30,** 765–775.

——, 1997: Contrail-cirrus and their potential for regional climate change. *Bull. Amer. Meteor. Soc.,* **78,** 1885–1903.

——, and C.-Y. Hsueh, 1998: Contrail properties derived from high-resolution polarization lidar studies during SUCCESS. *Geophys. Res. Lett.,* **25,** 1165–1168.

——, M. K. Griffin, and G. C. Dodd, 1989: Optical scattering and microphysical properties of subvisual cirrus clouds, and climatic implications. *J. Appl. Meteor.,* **28,** 91–98.

Schrader, M. L., 1997: Calculations of aircraft contrail formation critical temperatures. *J. Appl. Meteor.,* **36,** 1725–1728.

Schulz, J., 1998: On the effect of cloud inhomogeneity on area-averaged radiative properties of contrails. *Geophys. Res. Lett.,* **25,** 1427–1430.

Schumann, U., 1994: On the effects of emissions from aircraft engines on the state of the atmosphere. *Ann. Geophys.,* **12,** 365–384.

——, 1996: On conditions for contrail formation from aircraft exhausts. *Meteor. Z.,* **5,** 4–23.

——, and P. Wendling, 1990: Determination of contrails from satellite data and observational results. *Air Traffic and the Environment—Background, Tendencies and Potential Global Atmospheric Effects,* U. Schumann, Ed., Springer Verlag, 138–153.

Scorer, R. S., 1978: *Environmental Aerodynamics.* Ellis Horwood, 488 pp.

Seaver, W. L., and J. E. Lee, 1987: A statistical examination of sky cover changes in the contiguous United States. *J. Appl. Meteor.,* **26,** 88–95.

Sohn, B.-J., and E. A. Smith, 1992a: The significance of cloud–

radiative forcing to the general circulation on climate time scales—a satellite interpretation. *J. Atmos. Sci.,* **49,** 845–860.

——, and ——, 1992b: Global energy transports and the influence of clouds on transport requirements—a satellite analysis. *J. Climate,* **5,** 717–734.

Strauss, B., R. Meerkoetter, B. Wissinger, P. Wendling, and M. Hess, 1997: On the regional climatic impact of contrails—microphysical and radiative properties of contrails and cirrus. *Ann. Geophys.,* **15,** 1457–1467.

Travis, D. J., 1994: Jet aircraft condensation trails: Their radiative impacts and association with atmospheric conditions. Ph.D. dissertation, Indiana University, 118 pp. [Available from Dept. of Geography, Indiana University, Bloomington, IN 47405.]

——, 1996a: Diurnal temperature range modifications induced by contrails. Preprints, *13th Conf. on Planned and Inadvertent Weather Modification,* Atlanta, GA, Amer. Meteor. Soc., 110–111.

——, 1996b: Variations in contrail morphology and relationships to atmospheric conditions. *J. Wea. Modif.,* **28,** 50–58.

——, and S. A. Changnon, 1997: Evidence of jet contrail influences on regional-scale diurnal temperature range. *J. Wea. Modif.,* **29,** 74–83.

——, A. M. Carleton, and S. A. Changnon, 1997: An empirical model to predict widespread occurrences of contrails. *J. Appl. Meteor.,* **36,** 1211–1220.

Tselioudis, G., and W. B. Rossow, 1994: Multiyear variations of optical thickness with temperature in low and cirrus clouds. *Geophys. Res. Lett.,* **21,** 2211–2214.

——, A. A. Lacis, D. Rind, and W. B. Rossow, 1993: Potential effects of cloud optical thickness on climate warming. *Nature,* **366,** 670–672.

Twohy, C. H., P. A. Durkee, B. J. Huebert, and R. J. Charlson, 1995: Effects of aerosol particles on the microphysics of coastal stratiform clouds. *J. Climate,* **8,** 773–783.

Wagner, A. J., 1978: Weather and circulation of January 1978. *Mon. Wea. Rev.,* **106,** 579–585.

——, 1979: Weather and circulation of January 1979. *Mon. Wea. Rev.,* **107,** 499–506.

Wallace, J. M., and P. V. Hobbs, 1977: *Atmospheric Science: An Introductory Survey.* Academic Press, 467 pp.

Wang, P.-H., P. Minnis, M. P. McCormick, G. S. Kent, and K. M. Skeens, 1996: A 6-year climatology of cloud occurrence frequency from Stratospheric Aerosol and Gas Experiment II observations (1985–1990). *J. Geophys. Res.,* **101,** 29 407–29 429.

Wendland, W. M., and R. G. Semonin, 1982: Effect of contrail cirrus on surface weather conditions in the Midwest: Phase II. Final Report of NSF Grant ATM 8008812, Illinois State Water Survey, 95 pp. [Available from Atmospheric Sciences Division, Illinois State Water Survey, 2204 Griffith Dr., Champaign, IL 61820-7495.]

Wielicki, B. A., R. D. Cess, M. D. King, D. A. Randall, and E. F. Harrison, 1995: Mission to Planet Earth: Role of clouds and radiation in climate. *Bull. Amer. Meteor. Soc.,* **76,** 2125–2153.

Woodbury, G. E., and M. P. McCormick, 1986: Zonal and geographic distributions of cirrus clouds determined from SAGE data. *J. Geophys. Res.,* **91,** 2775–2785.